2019

Targeting Sphingosine Kinase 2 as a Treatment for Cholangiocarcinoma

Anthony D. Stillman
Human and Molecular Genetics

Targeting Sphingosine Kinase 2 as a Treatment for Cholangiocarcinoma

A thesis submitted in partial fulfillment of the requirements for the degree of Master of Science
at Virginia Commonwealth University

By

Anthony Dean Stillman

Bachelor's degree in Biology. University of Washington, Bothell, Washington, USA, 2015

Advisor: Huiping Zhou, Ph.D.

Professor, Dep, Department of Microbiology and Immunology

Virginia Commonwealth University

Richmond, Virginia

November 2019

Acknowledgment

I would like to acknowledge my PI, Dr. Huiping Zhou for helping me get through a tough point in my career and personal life. She took a risk by taking me in after my previous lab had left. Under her guidance, I improved my research and communication abilities. She gave me practical advice and reasonable objectives while pushing me forward. The lab also gave me a family away from home and this is not by accident. Dr. Zhou makes the lab feel like a family by encouraging teamwork, bringing food, having lunch celebrations for birthdays and individual's accomplishments, and lab trips. I highly appreciate how she has treated me and my fellow lab mates. I owe unmeasurable thanks to her.

I would also like to thank my fellow lab mates. They have been teachers and friends. They have helped me learn concepts, complete experiments, and have been supported during the long nights of research. Thank you all.

I want to show appreciation for my collaborators. I appreciate Dr. Guizhi Zhu and his graduate student Shurong Zhou for developing and producing the nanoparticles used in this study. I am thankful for Guanhua Lai help in diagnosing the human samples in my study.

And thanks to my committee members, Dr. Wang and Dr. Landry.

Table of Contents

List of Tables

List of Figures

List of Abbreviation

ABSTRACT

Targeting Sphingosine Kinase 2 as a Treatment for Cholangiocarcinoma

By Anthony Dean Stillman

A thesis submitted in partial fulfillment of the requirements for the degree of Master of Science at Virginia Commonwealth University.

Virginia Commonwealth University, 2019.

Major Director: Huiping Zhou, Professor, Department of Microbiology and Immunology

Cholangiocarcinoma (CCA) has a high mortality rate and its occurrence is rising. This increase prompts the need for improved CCA treatments. Studies have suggested that CCA is highly reliant on the sphingosine-1-phosphate-receptor-2 (S1PR2) and sphingosine kinase 2 (SphK2). Recently, a competitive SphK2 inhibitor, ABC294640, has been approved for clinical trial. ABC294640 has the potential to treat CCA, which is support by a phase I clinical study that was able to temporarily treat a patient suffering from metastasized CCA with ABC294640. To determine the viability of ABC294640 as a treatment for CCA, this study focused on determining the effects of ABC294640 on rat CCA cell lines. We found that ABC294640 inhibited the growth and migration of CCA and CAFs cells. The growth and count of 3-D organotypic co-culture of CCA and CAFs, which forms the "duct-like" structures, were reduced by ABC294640. The potential of inhibiting SphK2 as a treatment for CCA is supported by our finding of increased expression of S1PR2 and SphK2 in CCA patient liver samples. In conclusion, ABC294640 represents a potential therapeutic agent for CCA.

Chapter 1: Introduction

1.1 Cholangiocarcinoma and Risk Factors.

Cholangiocarcinoma (CCA) is the second most common form of liver cancer, behind hepatocellular carcinoma (HCC). In the United States, China, and Thailand there are 1.67, 17.5, and 60 per 100,000 people annually diagnosed with CCA, respectively (**Figure 1**). The rate of intrahepatic CCA (iCCA) diagnosed has been gradually increasing due to the changes in global dietary habits, population chemical exposure, and other factors[1]. Patients that are diagnosed with early-stage CCA have a 30% chance of surviving 5-year past their diagnosis with treatment, 20% of CCA cases are diagnosed at early stages. Patients with the late-stage diagnosis have ~2% of surviving 5-year past diagnosis even with treatment[2, 43]. The increasing global prevalence and the lack of effective treatment to combat the disease have created an urgent need for developing novel therapies for CCA.

CCA is derived from the cholangiocytes that make up the lining of the bile duct and its branches[1]. The liver synthesizes bile to be stored in the gallbladder. The bile duct transports bile from the liver/gallbladder to the intestine[3]. Due to CCA heterogeneous nature, its severity can be defined by CCA location within the bile duct system. The bile duct has two branches that reside within the liver, CCA that is found within those branches or are within the liver is referred as intrahepatic CCA (iCCA). CCA found in the first-half of the bile duct trunk below the bile duct branches is perihilar CCA (pCCA). The second half of the bile duct trunk can contain distal CCA (dCCA). The relative occurrence and 5-year survival rate of iCCA, pCCA, and dCCA is 10% and ~32.5%, ~65% and ~26%, and ~25% and ~27% respectively (**Figure 2**)[4]. The diagnosis rate of iCCA has been increasing[1].
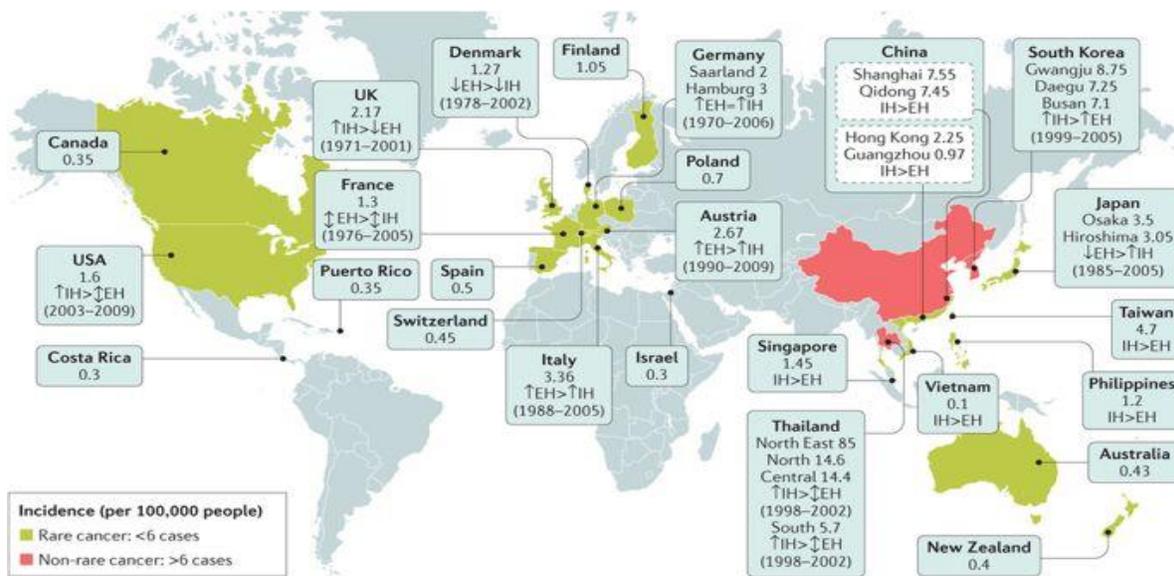
Figure 1: **Global Cholangiocarcinoma Incident Rate.** Numbers are cholangiocarcinoma cases per 100,000 people per region. Intrahepatic (IH) and extrahepatic (EH) cholangiocarcinoma with arrows indicating tempral trends of incident and greater sign indicates which form is most prevalent.[1]
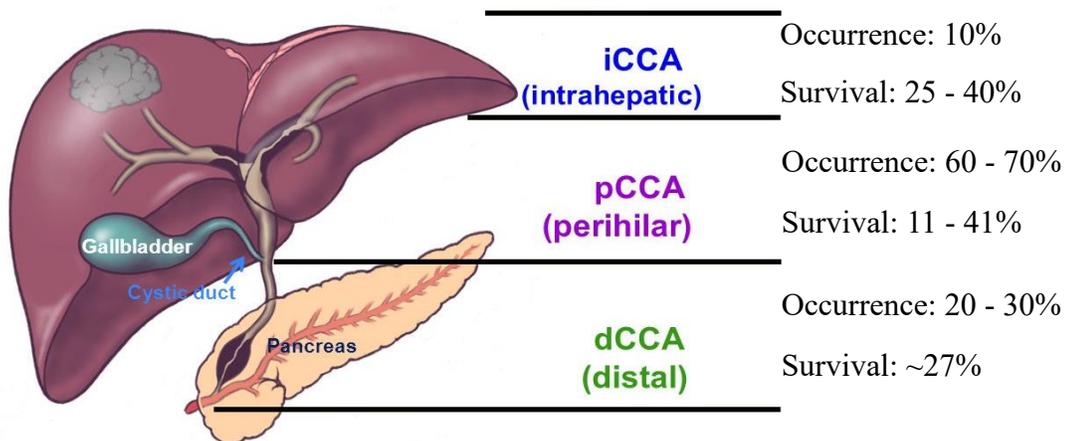
Figure 2: **Classification of Cholangiocarcinoma.** Types of cholangiocarcinoma (CCA) with associated relative occurrence and 5-year survival expectancy[4].

The global diagnosis rate of CCA is gradually increasing[1]. This is due to improvement in diagnosis methods, an increase of individuals with established risk factors, and the emergence of new risk factors[1]. Until recently, CCA occurred in very specific parts of the world, namely north Thailand and southern China. The reason for the locality of the disease is due to the very specific environmental factor of *fasciola hepatica* (Liver Fluke), a parasite that infects and grows in human livers, causing liver fibrosis. Liver fibrosis increases the risk of developing CCA[1].

Many CCA risk factors induce liver fibrosis. Factors that induce liver fibrosis are primary sclerosing cholangitis, toxins (alcohol), liver cirrhosis, and HCV. Other risk factors are bile duct cysts, bile duct stone, inflammatory bowel disease (IBD), obesity, and diabetes (**Figure 3**)[1,4]. Out of these risk factors, obesity and diabetes have had the most significant global increase over recent times[5,6], which can explain why CCA rates have been increasing outside of east Asia[1].

1.2 Cholangiocarcinoma Treatments.

The current treatment for CCA is limited. Radiation, chemotherapy, and surgery each give patients a 20% chance of surviving 5-year past diagnosis[9,10,11]. The combination of these conventional treatments can increase a patient's survival chances to 70%[9]. Treatments more specific for CCA involve surgically replacing portions of the liver and bile duct system. The most successful specific procedure for CCA is liver transplant increasing the patients' 5-year survival chances to 53%[8]. The effectiveness of this procedure is for two major reasons. The patient's possibly cancer infiltrated liver being removed, also removing the metastasized cancer. And one of the major factors that promote the spread of CCA is a diseased liver, thus replacing the patient's unhealthy liver with a healthy liver decreases the progression of CCA. Liver transplants are rarer and far more effective then bypass procedures, which have a 5-year survival rate of ~0%[12,13]. These bypass procedures are invasive and are implemented in patients

4
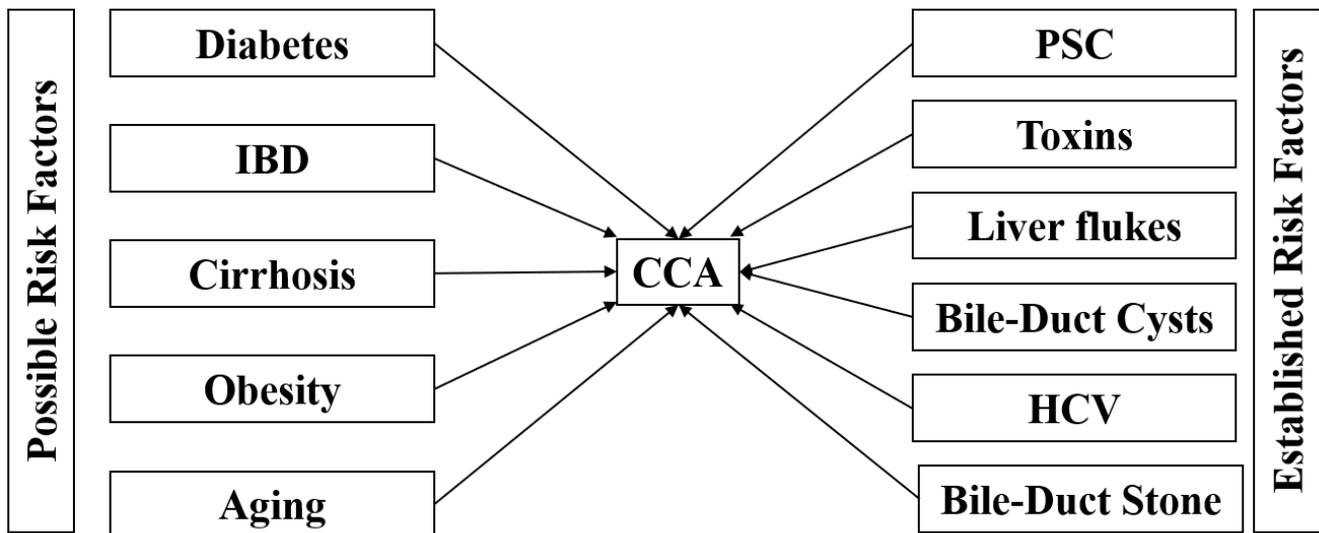
Figure 3: **Risk Factors.** The established and possible risk factors that assist the progression of Cholangiocarcinoma (CCA). Risk factors are linked to liver disease[1,4].

with late-stage CCA, thus these procedures only extend patient survival slightly. The biliary bypass is removing the bile duct and replacing it with a portion of the gut[12]. Stent placement is replacing the bile duct with a polymer tube[13]. The reason for the effectiveness of bypasses is it removes the source of CCA, the bile duct, and stopping bile acids from reaching CCA and cholangiocyte cells (**Figure 4**).

The rise of CCA occurrence and CCA risk factors has prompted a response by the medical community, which has increase diagnosis methods of CCA. The ability to diagnosis CCA has been improved by the addition of endoscopic ultrasound and blood tests for liver function and tumor antigens[7]. Even with these additional tools, few CCA cases are caught at early stages when treatment is the most effective[7]. For the sake of global health, new novel medicines to treat late-stage CCA need to be developed.

1.3 Bile Acids.

Bile acids are a class of zwitterionic ligands/detergent produced in the liver[14]. Bile acids are stored in the gallbladder and transported down the bile duct and through the gut to act as detergents to help to solubilize the lipids and absorb nutrition [15]. Once the bile acids have reached the ileal, enterohepatic circulation transports 95% of the bile acids back to the liver to be reused, via the portal venous system[18]. While on this journey, bile acids can be conjugated into conjugated bile acids (CBA) in the liver and deconjugated by bacteria in the colon. Glycocholic acid (GCA) and taurocholic acid (TCA) are the two major primary bile acids. These CBAs endocrinologically affect different types of cells throughout the liver and gut axis (**Figure 5**)[15]. The cholangiocytes and myofibroblasts that make up the bile duct possess cell surface receptors

that can be activated by CBA. The cellular response is based on the ratio of CBA and their target receptors the cell possesses[19,20]. The most prevalent CBA receptor are sphingosine-1-phosphate

Survival Rate: 0%[12]

Survival Rate: 0%[13]

Survival Rate: 53%[8]

Biliary bypass

Stent placement

Liver transplant

Treatment for CCA

Surgery

Chemo-therapy

Radiation

Survival Rate: 20%[11]

Survival Rate: 20%[10]
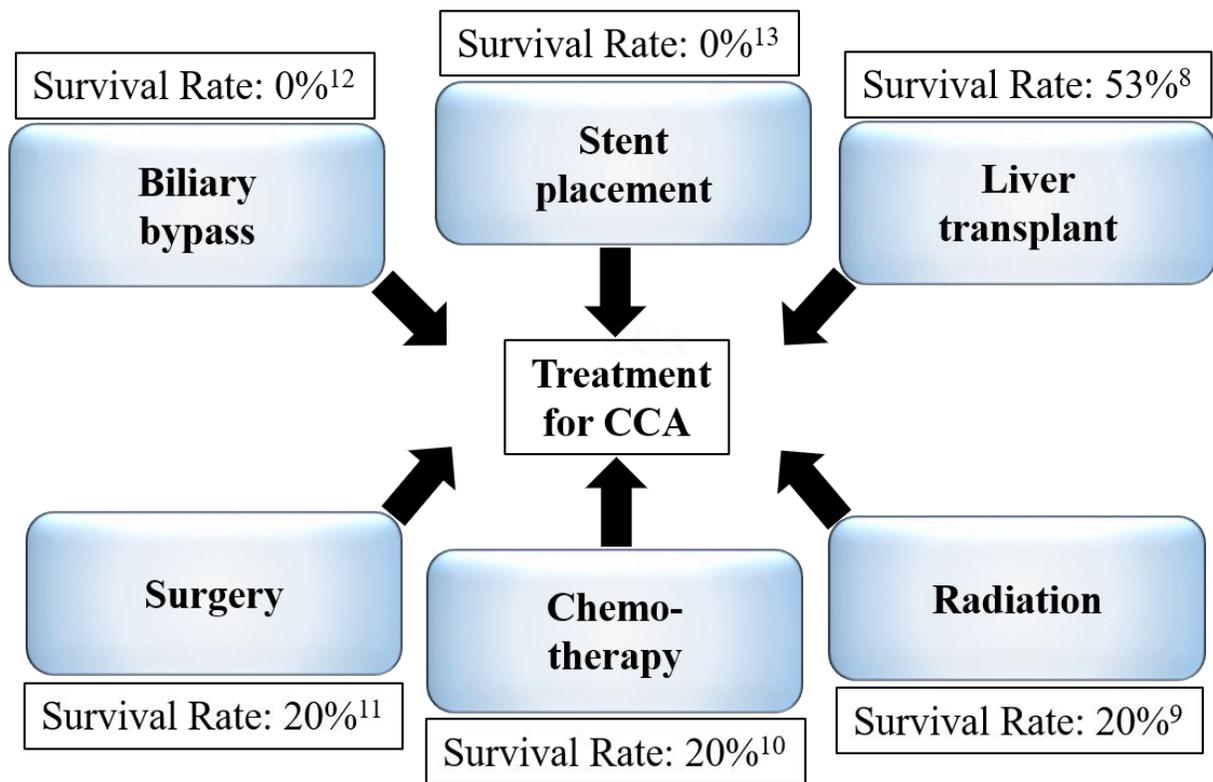
Survival Rate: 20%[9]

Figure 4: **Treatments of Cholangiocarcinoma**. Various types of treatments for cholangiocarcinoma (CCA) and the associated 5-year survival rate after diagnosis with treatment.[9,8,10,11,12]
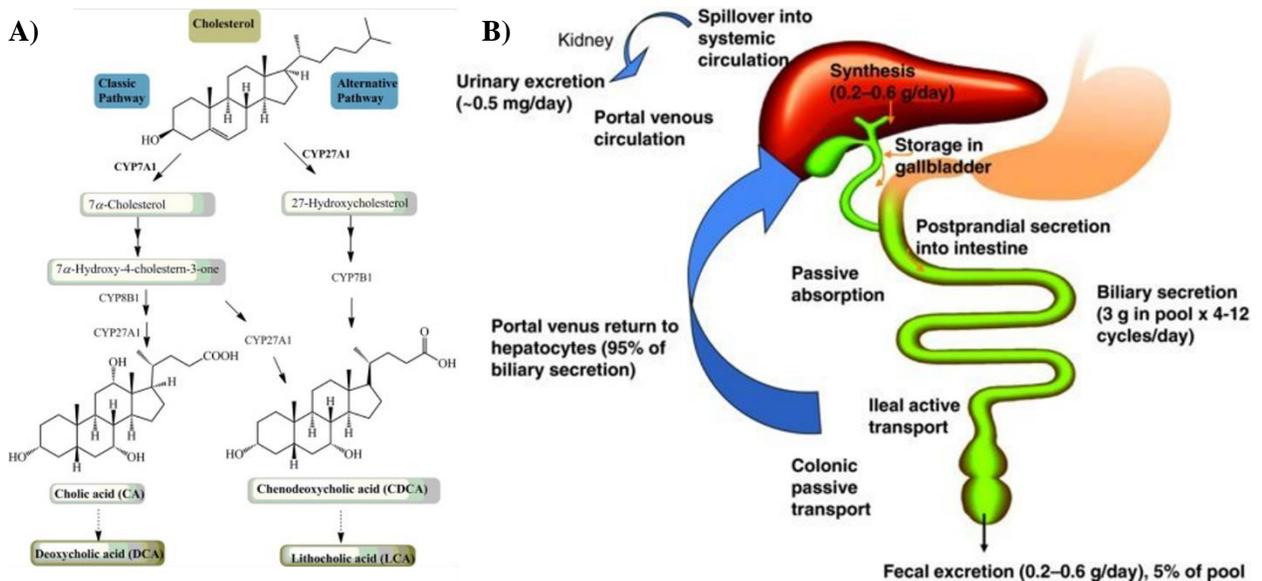
Figure 5: **Bile-Acid synthesis and Intrahepatic Transport. A)** Bile acid synthesis and conjugation that occurs in the liver. **B)** Intrahepatic circulation that transports the bile acids down the bile duct/gut followed by transport of bile acid through the ileum into the portal venous system. The portal venous system transports 95% of the bile acids to the liver for reuse[38,37].

receptor 2 (S1PR2)[19]. This receptor is critical in CBA-induced CCA cell metabolism, proliferation, and migration.

1.4 S1PRs and Sphingosine Kinase 2 (SphK2) Pathway.

There are five sphingosine-1-phosphate receptors (S1PR1-5) and their expression varies on cell types. S1PRs have many downstream targets, making it difficult to target these receptors as a treatment without unwanted side effects[21]. The most prevalent of these receptors in the liver/bile duct is S1PR2[22]. Both cholangiocytes and the myofibroblasts of the bile duct possess S1PR2 on their cell surface[19,20]. S1PR2 are G-protein-coupled receptors (GPCRs)[22]. GPCRs are a large family of transmembrane receptors. GPCR is composed of an extracellular surface ligand-binding domain and an intracellular guanine nucleotide exchange factor (GEF); which is also composed of a complex of α, β, and γ subunits[24]. When a CBA or S1P binds to S1PR2, it induces a conformation change that activates the GEF. The activated GEF supplants the GDP on the α-subunit with a GTP, allowing it to disassociate from the β and γ subunits. The disassociated subunits induce a reaction across the cell surface-associated proteins leading to the activation of the epidermal growth factor receptor (EGFR)[24]. EGFR activates the MAPK/ERK pathway, causing the phosphorylation of ERK1/2 into p-ERK1/2. The p-ERK1/2 is transported to the nucleus where it phosphorylates SphK2 at ser-351 into p-SphK2[25]. Activated SphK2 generates nuclear S1P, which is a powerful inhibitor of HDAC1/2[26]. The inhibition of HDAC1/2 by S1P leads to increasing histone acetylation causing epigenetic changes and altering gene expression (**Figure 6**)[27,42]. The activation of S1PR2 in CCA drives the progression of cancer via SphK2 and
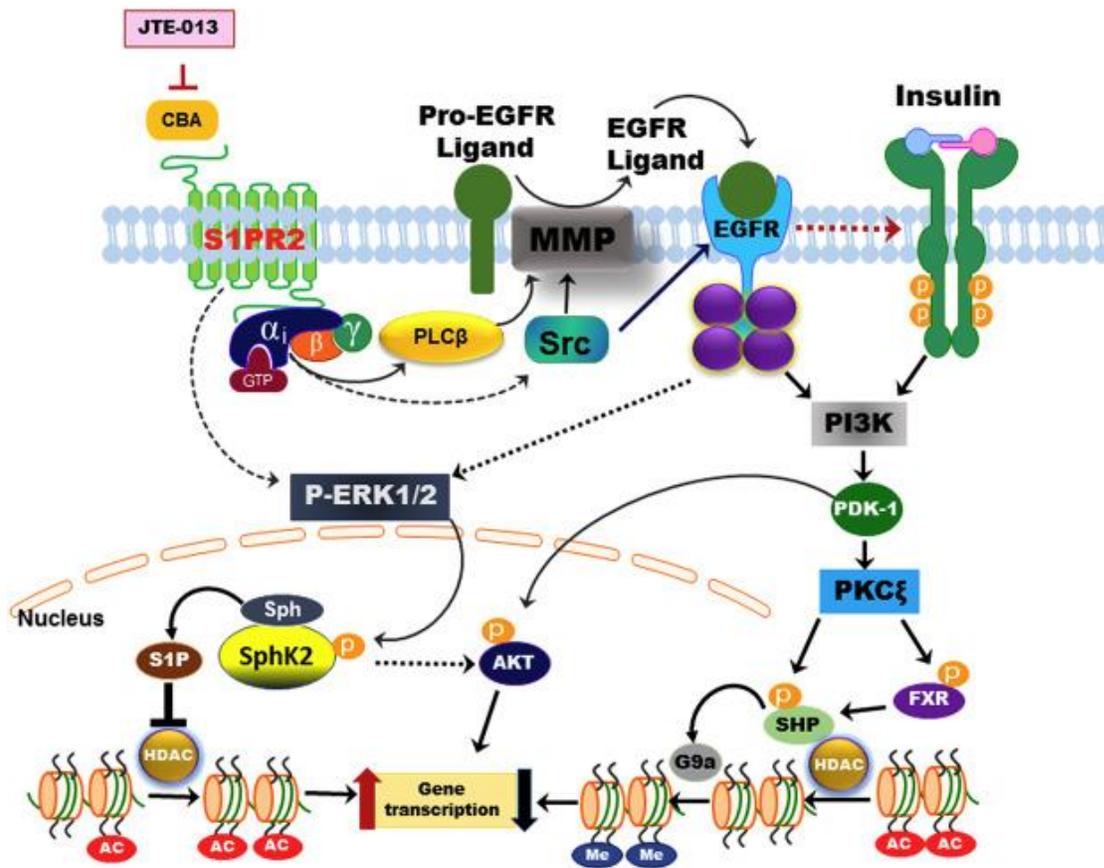
Figure 6: **S1PR2/ERK/SphK2 Pathway.** Conjugated bile-acid (CBA) activates sphingosine-1-phophate receptor 2 (S1PR2). S1PR2 G-protein-coupled complex releases the alpha-subunit (α_1) which activates phospholipase C-beta (PLCβ) and Src kinase. This leads to the activation of matrix metallopeptidase, which partially degrades Pro-EGFR ligand. The ligand binds epidermal growth factor receptor (EGFR) allowing it to assist S1PR2 activate extracellular signal-regulated kinases 1/2 (ERK1/2). ERK1/2 enters the nucleus and phosphorylates sphingosine kinase 2 (SphK2). SphK2 phosphorylates sphingosine (Sph) into sphingosine-1-phosphate (S1P). S1P inhibits HDAC1/2 increasing histone acetylation thus altering gene expression[42].

other pathways[27,28]. These pathways increase cell growth, proliferation, and metabolism[27]. The most impactful and enduring effect is the epigenetic alterations incurred by SphK2. Increase activity of SphK2 has been linked to increases in neoplastic transformation, tumorigenesis, migration, proliferation, metastasis, metabolism, drug resistance, and overall cancer progression[27, 44 - 46]. The effect of SphK2 on cell proliferation is not limited to CCA cells, it also affects the cancer-associated myofibroblasts (CAFs) that support CCA may use the S1PR2/ERK/SphK2 pathway to progress the tumor microenvironment.

Tumor cells can recruit surrounding cells for support. A major group that supports CCA tumors are CAFs. CCA cells release various ligands to recruit CAFs for assistance. CAFs perform activities that are crucial for the survival, progression, and metastasis of the CCA tumor[41,29]. Especially α-SMA positive CAFs, which have a positive correlation with tumor size and negative correlation with patient survival[41]. The CAFs promote the tumor via altering the tumor microenvironment and promoting the cancer cell growth directly, essentially assisting the CCA to achieve the various hallmarks of cancer. To induce angiogenesis, the CAFs release cytokines that attract macrophages to assist in angiogenesis. The CAFs surround the cancer cells, sheltering the tumor from an immune response. CAFs promote CCA growth by releasing growth factors and directly interacting with the CCA cells. Once the tumor is large enough, the CAFs release proteins that break down the extracellular matrix around the tumor, releasing the CAFs and the contained CCA cells away from the surrounding tissue leading to metastasis. The cooperation of the CAF cells with the CCA tumor is necessary for the progression of the cancer[30].

CCA cells communicate with the CAFs via various signaling pathways. CCA cells excrete S1P at a heightened rate compared to healthy cholangiocytes[31]. This unusual high levels

of S1P in the tumor microenvironment is known to promote CCA cell growth and most likely induces cancer-promoting behavior from CAFs[29]. This is supported by the presence of S1PR2 in CAF cells[20]. The presence of S1PR2 in the CAFs also allows for CAFs to be promoted by CBA that pass through the bile duct. This sensitivity to CBA is particularly crucial due to CCA and CAFs tumor masses blocking the bile duct, causing a backup and buildup of CBA around the tumor[32]. The backup increases the concentration of CBA around the tumor, promoting tumor growth via the S1PR2/ERK/SphK2 pathway[32]. S1PR2/ERK/SphK2 pathways importance to CCA/CAFs tumor growth, communication, and metastasis makes it a prime target for cancer treatment (**Figure 7**). Due to S1PR2 and ERK importance to other pathways, targeting them would have off-target effects. SphK2 is at the end of the pathway, making it a prime target for treatment.

SphK2 is an enzyme that binds and phosphorylates sphingosine into S1P. SphK2 kinase function is primarily performed in the nucleus, as discussed before[26]. SphK2 has a sister protein that resides in the cytoplasm, SphK1. The SphK1/2 sister enzymes have very similar structures at their kinase active sites with the main difference between the sisters being in the length and composition of their c-terminuses, which determines the kinases locality within the cell. When activated, SphK1 binds to the interior of the cell membrane to produce S1P[33]. When SphK2 is inhibited, the activity and quantity of SphK1 are upregulated within the cell to seemingly maintain healthy extracellular and cytoplasmic S1P levels[34]. This is crucial due to the overall importance of S1P in the cytoplasm and blood/lymph for the normal function of the body. Thus,
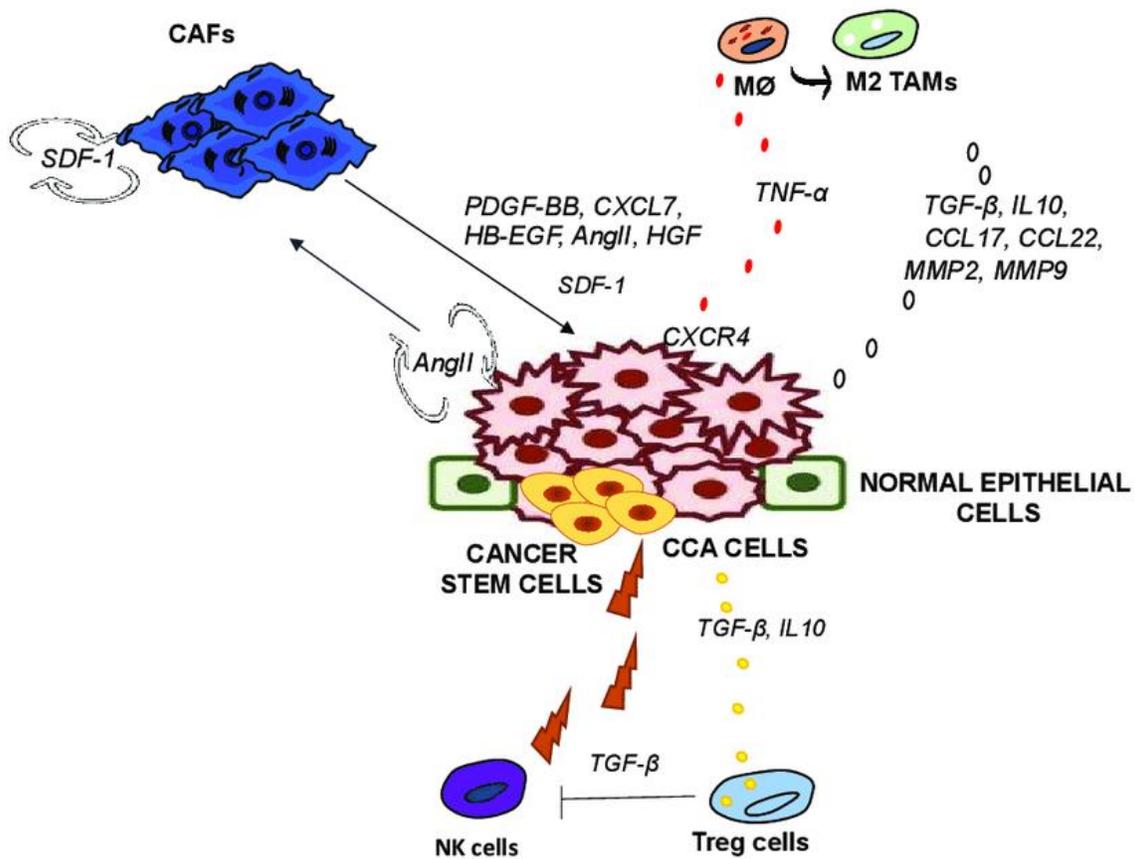
Figure 7: **Cancer-Associate Myofibroblasts of Cholangiocarcinoma.** Cancer-associated myofibroblasts (CAFs), cholangiocarcinoma (CCA), and other cells types endocrine communication, modifying the cancer microenvironment[39].

inhibiting SphK2 will only lead to a decrease of S1P in the nucleus and not the rest of the body. SphK1 compensation of S1P while SphK2 is inhibited further limits the possible side effects of inhibiting SphK2, increasing SphK2 lure as a target for CCA treatment. There are several SphK2 inhibitors available.

1.5 SphK2 inhibitors.

Extensive efforts have been made to develop specific SphK2 inhibitors. Most of the inhibitors bind both SphK1 and 2, due to the similar structures[35]. Recently isotype-specific inhibitors have been developed. The most promising of these compounds is ABC294640, which is a competitive inhibitor (**Figure 8**). ABC294640 has already been approved for the clinical trial. ABC294640 treatment can be taken orally in 250 mg dosage (~ 7 µM) with limited side effects[36]. A phase I study on a group of patients with various forms of cancer was conducted with ABC294640. Out of the various types of cancers, the patient with metastatic CCA had the most positive outcome[47]. The mechanism of how ABC294640 affects CCA is still being explored. Recently, a human intrahepatic CCA cell study was conducted to determine the mechanism ABC294640 inhibited CCA. The study showed that ABC294640 stopped SphK2 inhibition of NOXA production. NOXA inhibits MCL1, an anti-apoptotic protein that is a part of the BCL2 family, thus increasing cell apoptosis. The study concluded ABC294640 indirectly induced apoptosis through the promotion of NOXA production. The study also showed that BCL2 family inhibitors synergized with ABC294640 to increase CCA apoptosis[48]. The study results are promising but did not include a healthy control cell line and their 50 µM ABC294640 dosage is far above the clinical standard. Further research needs to be done to better understand how ABC294640 effects CCA. A more potent sphK2 inhibitor is K145 hydrochloride (K145). K145

14
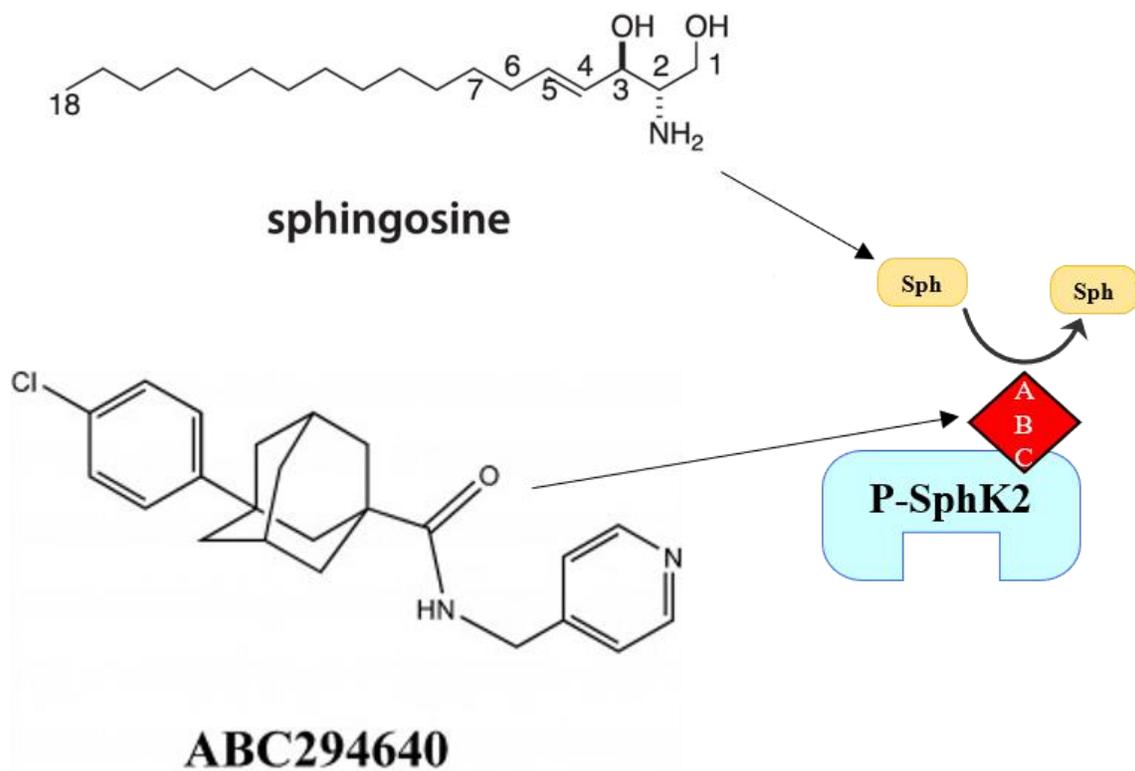
Figure 8: ABC294640 Mechanism on Sphingosine Kinase 2. ABC294640 is a competitive inhibitor for sphingosine kinase 2 (SphK2). ABC294640 binds the phosphorylation site of SphK2, blocking sphingosine (Sph) from entering the site, thus halting the creation of sphingosine-1-phosphate (S1P)[48].

has not been approved for clinical use and has the same competitive inhibitor traits as ABC294640, but is more toxic to cells[51].

1.6 Nanoparticle Drug Delivery.

ABC294640 hydrophobic structure impedes its transport through the body, which can be circumvented by Nanoparticle drug delivery. Nanoparticles are micelle like structures made of various smaller artificial constructs[41]. This artificial construction makes the nanoparticles highly customizable; the customizable traits are as follows[41]. Nanoparticles are generally 100 to 500 nm in diameter; the size of a nanoparticle structure dictates its ability to pass through a cell membrane[41]. The interior of the nanoparticle can be modified to be able to seat specific particles for transport[41]. The exterior of a nanoparticle can possess antibodies or other structures that help guide the particle to cancer. Once the nanoparticle is inside the cell, it can gradually or immediately release its content inside the cell (**Figure 9**)[41]. The nanoparticle can be designed to contain one or multiple drugs[41]. All these traits make nanoparticles a great partner for ABC294640 delivery.

16
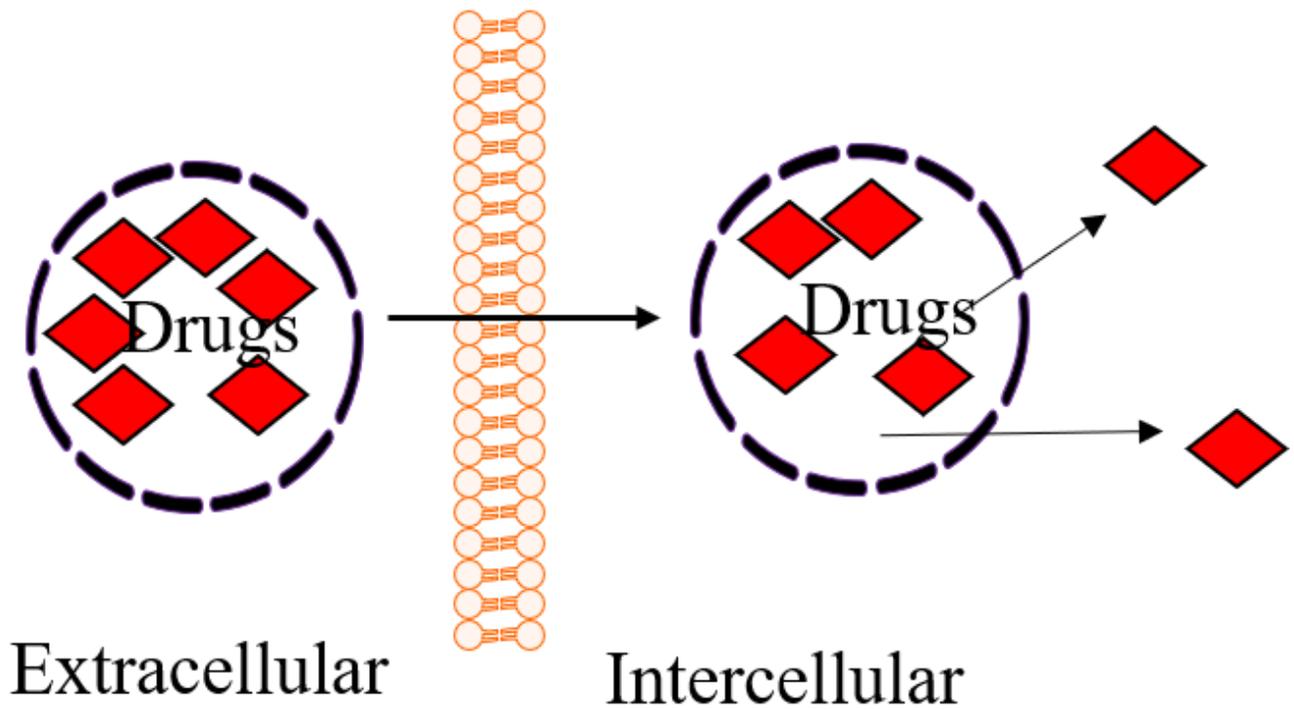
Figure 9: **Nanoparticle Drug Delivery.** Drugs encapsulated in nanoparticle micelle constructs for transport into the cell and drug release.

Chapter 2: Materials and Methods

2.1 Materials.

- Trypsin-EDTA, (Gibco, ThermoFisher, 25200056)

- Dulbecco's Modified Eagle Medium (DMEM), (Gibco, 11995-065)

- Fetal Bovine Serum (FBS), (Sigma, F2442)

- Penicillin Streptomycin (P/S), (ThermoFisher, 15140122)

- Phosphate Buffer Solution (PBS), (Sigma-Aldrich, P5494)

- Insulin, 100 units per 100Ml

- Dimethyl Sulfoxide (DMSO), (Sigma-Aldrich, D2650)

- Trypan Blue, (Sigma-Aldrich, T8154)

- Ammonium Persulfate, (Sigma-Aldrich, A3678)

- 30% Acrylamide/Bis Solution 29:1, (BIO-RAD, 1610156)

- TEMED (BIO-RAD, 161-0800)

- SDS, (sodium dodecyl sulfate, L4509)

- HEPES, (4-(2-hydroxyethyl)-1-piperazineethanesulfonic acid, Sigma-Aldrich, H-9136)

- KCl, (potassium chloride, Sigma-Aldrich, P-3900)

- EDTA, (Ethylenediaminetetraacetic acid, Sigma-Aldrich, ED4S)

- EGTA, (Ethylene glycol-bis(2-aminoethlether)-N,N,N',N'-tetraacetic acid Sigma-Aldrich, E0396)

- NaF, (Sodium Fluoride, Sigma-Aldrich, S-1594)

- Na3VO4, (Sodium orthovanadate, Sigma-Aldrich, S6508)

- Leupeptin, (Sigma-Aldrich, 103476-89-7)

- Aprotinin, (Sigma-Aldrich, 9087-70-1)

- Pepstatin A, (Sigma-Aldrich, 26305-03-3)

- PMSF, (Phenylmethanesulfonyl Fluoride, Sigma-Aldrich, P7626)

- NaCl, (sodium chloride, ThermoFisher, S641-212)

- Tergitol^{TM} Solution (NP-40), (Sigma-Aldrich, 1002526600)

- β-Glycerol phosphate, (Sigma-Aldrich, G-6251)

- Glycerol, (Sigma-Aldrich, 56-81-5)

- Benzamidine, (Sigma-Aldrich, 206752-36-5)

- BIO-RAD Protein Assay Dye Reagent Concentrate, (BIO-RAD, 5000006)

- Precision Plus Protein^{TM} Dual Color Standards, (BIO-RAD, 161-0374)

- Nitrocellulose Membrane Roll, (GVS North America Sanford, 1215471)

- Tris base, (Trizma Hydrochloride, Sigma-Aldrich, T3253)

- Glycine, (Sigma-Aldrich, G-8898)

- Methanol, (Fisher, A454-4)

- Dry-Milk

- BSA, (Bovine Serum Albumin, Sigma, B4287)

- Tween$^{®}$-20, (Sigma-Aldrich, 9005-64-5)

- ECL, (PerkinElmer, ORT2655)

- TRIzol, (TRI-Reagent$^{®}$, Sigma-Aldrich, T9424)

- Chloroform, (Sigma-Aldrich, 67-66-3)

- 2-propanol, (Sigma-Aldrich, I9516)

19

- Ethanol, (Koptec, 64-17-5)

- High-Capacity cDNA Reverse Transcription Kit, (ThermoFisher, 4368814)

- iQTM SYBR Green Supermix reagents

- Formaldehyde, (Sigma-Aldrich, 252549)

- Collagen I, Rat Tail, (Corning®, 354236)

- NaOH, (Sodium hydroxide, Sigma-Aldrich, 7647-14-5)

- Xylenes, (Histoprep, 1330-20-7)

- Hydrogen peroxide, (Sigma-Aldrich, 216763)

- Na2HPO4, (Sodium phosphate dibasic, Sigma-Aldrich, 7558-79-4)

- KH2PO4, (Potassium phosphate monobasic, Sigma-Aldrich, 7778-77-0)

- H&E staining kit, (Hematoxylin and Eosin, Abcam, ab245880)

- VECTASTAIN® ABC HRP Kit (Peroxidase, Rat IgG, VectorLab, PK-4004)

- DAB Peroxidase (HRP) Substrate Kit (with Nickel), 3,3'-diaminobenzidine (VectorLab, SK-4100)

- VECTASHIELD® Hardset™ Antifade Mounting Medium with DAPI (VectorLab, H1500)

- CCK-8, (Cell-Counting Kit-8, Dojndo, CK04)

- ABC, (ABC294640, Selleckchem, S7174)

- TCA, (Sodium Taurocholate Hydrate, Sigma-Aldrich, 345909)

- Triton™ 100 (Sigma-Aldrich, T9284)

2.2 Solutions and Buffers.

2.2.1 Buffer A: 10 mM, 7.4 pH, HEPES, 10 mM KCl, 0.1 mM EDTA, 0.1 mM EGTA, 2 mM NaF, 2 mM, 25 µg/mL leupeptin, 25 µg/mL aprotinin, 10 µg/mL pepstatin A6305-03-3), and 0.1 mM PMSF.

2.2.2 Buffer B: 20 mM, 7.4 pH, HEPES, 0.4 M NaCl, 1.0 mM EDTA, 1.0 mM EGTA, 2mM NaF, 2 Mm Na_3VO_4, 25 µg/mL leupeptin, 25 µg/mL aprotinin, 10 µg/mL pepstatin A, and 0.1 mM PMSF.

2.2.3 Total: 25 mM, 7.4 pH, β-Glycerol phosphate, 5 mM EDTA, 5 mM EGTA, 25 mM NaF, 1mM Na_3VO_4, 1.0% triton X-100, 0.1.0% SDS, 10% glycerol, and 5 mM benzamidine.

2.2.4 AP:1.0 g ammonium persulfate dissolved in 10 mL of ddH_2O.

2.2.5 SDS: 10 g Sodium dodecyl sulfate dissolved in 100 mL of ddH_2O.

2.2.6 Running Buffer x5: 125 mM Tris base, 2.5 M Glycine, SDS 5 g/mL. pH 7.4.

2.2.7 Running Buffer: 200 mL of running buffer x5 and 800 mL of ddH_2O.

2.2.8 Transfer Buffer x10: 1.92 M glycine and 250 mM tris base. pH 7.4.

2.2.9 Transfer Buffer: 100 mL of transfer buffer x10, 700 mL of ddH_2O, and 200 mL of Methanol.

2.2.10 TBS x10: 100 mM Tris base and 1.5 M NaCl. pH 7.4.

2.2.11 TBST: 100 mL of TBS x10, 900 mL of ddH_2O, and 1 mL tween®-20.

2.2.12 1 mM EDTA: 372 mg of EDTA dissolved in 1 mL of ddH_2O. pH 8.0.

2.2.13 PBS x10: 80 g of NaCl, 2.0 g of KCl, 14.4 g of Na2HPO4, and 2.4 g of KH2PO4 dissolved in 1.0 L. pH 7.5.

2.2.14 PBST: 100 mL of PBS x10, 900 mL of ddH_2O, 1 mL of tween®-20.

2.2.15 2.5% BSA-PBS: 0.2% triton X-100 and 2.5% BSA in PBS buffer.

2.3 Cell Culture.

2.3.1 Cell lines: Five ratcell lines were used for the various experiments in this study. BDE1 cells are a immortalized non-tumorigenic cell line that represents the normal bile duct cholangiocytes cells. The following cell lines were BDEsp tumor-derived. BDEsp-TDF$_{E4}$ cancer-associated myofibroblasts (CAFs) cell line (clone E4) and BDEsp-TDE$_{H10}$ cholangiocarcinoma (CCA) cell line (clone H10). These two cell lines were extracted from the same tumor and cooperate with each other. A more aggressive forms of BDEsp-TDE cell line are BDEsp-TDE$_{neu}$ and BDEsp-TDE$_c$. BDEsp-TDE$_{neu}$ cells have a mutation in the HER2 gene, increasing the receptors expression and BDEsp-TDE$_c$ is the same cell line, without the mutation.

2.3.2 Cell Medium: 450 mL of DMEM GIBCO medium, 50 mL of fetal bovine serum (FBS), 5 mL of penicillin-streptomycin, 3.48 mg of transferrin, and 97 µL of insulin were mixed. The solution was filtered and added to 500 mL of DMEM GIBCO medium to create 10% FBS medium. 01% FBS medium contains 10 mL of FBS and instead of 50 mL of FBS. The medium was stored at 4 °C and warmed in 37 °C water bath before use.

2.3.3 Cell Culture: All BDEsp cell lines were cultured in 10 mL of DMEM GIBCO medium with 10% FBS, 1% penicillin-streptomycin, 1 µmol/L of insulin, and 5 µg/mL of transferrin. The cells were incubated at 37 °C and 5.0% CO_2 in a humidified cell culture incubator.

2.3.4 Cell Sub culturing: Cells were allowed to incubate and divided in 100 mm plate until reaching 70% to 90% confluency, 3 to 4 days. In cell-hood, the medium was removed from the plate and 3 mL of trypsin was added. The plate was placed in the 37 °C cell incubator for 3 to 5 minutes. Detached cells were washed off plate with trypsin and added to warm medium equal to trypsin in volume, to deactivate the trypsin. The medium was centrifuge for 5 minutes at 1350

rpm. The medium was aspirated from cell pellet. Cells were suspended in fresh warm medium and added to 100 mm cell plates containing 10 mL of warm DMEM medium. The cells were incubated at 37 °C and 5.0% CO2 in humidified cell culture incubator.

2.3.5 Freezing: $1.0*10^6$ Cells were suspended in 20% FBS, 10% DMSO, and 70% cell medium to a final volume of 1.5 mL. The solution was added to cryotube and placed in -80 °C storage for 3 to 5 days. Then the cells were transferred to liquid nitrogen tanks for long term storage.

2.3.6 Thawing: Frozen cells were kept in cryotube and stored in liquid nitrogen. Once removed from liquid nitrogen, cryotube containing cells are incubated in 37 °C water bath for one minute, to thaw cells. The cryotube was taken into cell-hood and cell solution was transferred into 3 mL of warm medium. The medium was centrifuge for 5 minutes at 1350 rpm. In the cell-hood, medium was removed from the cell pellet. Cells were suspended in fresh warm medium and added to 100 mm cell plates containing 10 mL of warm medium. Cells were incubated overnight at 37 °C. After overnight incubation, the medium was refreshed and the incubation of the cells resumed.

2.4 Western Blot Analysis.

2.4.1 Cytosol and Nucleoplasm Protein Lysate Extraction: Cells in a 60 mm plate at 80% to 90% confluency were washed with 6 mL of cold PBS 3 times. 400 µL of buffer A was added to plate to cover cells. Cells were scraped off the plate and pipette into 1.5 mL tube. The solution was vortexed for 10 seconds and incubated for 15 minutes on ice. 25 µl of 10 % NP-40 is added to solution and vortex for 10 seconds, then incubate on ice for 30 minutes. In 4 °C, centrifuge for 1 minute at max speed. Collect cytosol supernatants from nucleus pellet. Resuspend the nuclear fraction in 30 µl of buffer B with pipette. Vigorously shake the tubes for 20 minutes at 4 °C on

shaking platform. Spin at 4,000 rpm at 4 °C for 5 minutes. Transfer the nuclear fractions to clear tubes. Measure protein concertation and store at -80 °C.

2.4.2 Cell Total Protein Lysate Extraction: Cells in a 60 mm plate at 80% to 90% confluency were washed with 6 mL of cold PBS, pH 7.4, 3 times. 200 µl of total protein lysis buffer was added to cover cells. Cells were scraped off the plate and pipette into 1.5 mL tube and vortexed for 10 seconds. Freeze cells at -80 °C for 2 hours. Thaw solutions on ice and centrifuge at 12,000 rpm for 10 minutes. Collect lysate and transfer to final tube. Measure protein concentration and store at -80 °C.

2.4.3 Tissue Total Protein Lysate Extraction: Add 50 mg of tissue into 1 mL of total protein lysis buffer. Homogenize Tissue with Precellys Evolution Homogenizer, Bertin Technologies (P000062-PEV00-A). Freeze cells at -80 °C for 2 hours. Centrifuge samples at 12,000 rpm for 10 minutes. Collect lysate and transfer to the final tube. Measure protein concentration and store at -80 °C.

2.4.4 Measuring Protein Concentration: Mix assay solution of 1-part Protein Assay Dye and 4-parts deionized water. Aliquot assay solution into 500 µL fractions in 1.5 mL tube. Pipette 1.0 µL of protein solution into assay solution fraction and mix. Pipette 200 µL of the mixture into 2 wells of 96-well plate. Pipette 200 µL of assay solution into 2 wells of 96-well plate; this will act as a negative control. Measure wells absorbance at 600 nm. Calculate protein concentration.

2.4.5 Protein Gel Electrophoresis: A fraction of protein solution containing a sum of 35 µg of protein was add to a 1.5 mL tube. The fraction was then diluted with ddH$_2$O and 10 µL XT sample buffer x4 to a final volume of 40 µL. The mixture was then incubated in heating block at 100 °C for 15 minutes to denature the protein. Denatured samples were incubated on ice or stored at -20 °C until gel is prepared. Protein gels were fixed to western electrode chamber and

placed in electrophoresis tank. Chambers and tank were filled with running buffer solution. Precision Plus Protein™ Dual Color Standard is added to book-ending wells of the gel. Denatured protein fractions were pipetted into wells. Electrophoresis was started at 80 V for 15 minutes and the rest of the run was done at 120 V. Run was complete when ladder reached the bottom of the gel.

2.4.6 Gel to Membrane Protein Transfer: Protein was transferred from gel to nitrocellulose membrane using a wet transfer method. Gel and membrane were sandwiched together in a cassette with foam pad and filter paper. Cassette was placed in buffer tank and tank was filled with transfer buffer. Protein was then transferred from gel to membrane with 0.32 W current for 80 minutes while kept cold.

2.4.7 Membrane Blocking: Once the protein has been transferred, the nitrocellulose membrane was placed in container filled with TBST. 5.0% milk blocking solution was created by mixing 5.0 g of dry milk into 100 mL of TBST. The TBST was poured off the membrane and blocking solution was added. Blocking was done for 2 hours at room temperature (RT) on rocker.

2.4.8 Primary Antibody Incubation: 1.0% BSA solution is composed of 1.0 g of bovine serum albumin (BSA) in 100 mL of PBST buffer. Primary antibody solution is 1:1000 or 1:500 antibody dilution in 1.0% BSA solution. Membranes were submerged in primary antibody solution and incubated overnight on a rocker at 8 °C. After incubation, membranes were washed with TBST three times at room temperature (RT) on rocker for 15 minutes each.

2.4.9 Secondary Antibody Incubation: 1.0% BSA solution is composed of 1.0 g of bovine serum albumin (BSA) in 100 mL of TBST buffer. Secondary antibody solution is 1:1000 antibody dilution in 1.0% BSA solution. Membranes were submerged in secondary antibody

solution and incubated for 1 hour on a rocker at RT. After incubation, membranes were washed with TBST three times at room temperature rocker for 15 minutes each.

2.4.10 Imaging proteins: After residual secondary antibody is washed off, the membranes were imaged. Membranes were dried and placed in Bio-Rad Gel Doc XR+ Imaging System. Enhanced luminol-based chemiluminescent (ECL) was added to the surface of the protein and images were taken with optimal system settings.

2.5 3-D Organotypic Culture Model of Cholangiocarcinoma.

2.5.1 3-D Organotypic BDEsp-TDF$_{E4}$ and BDEsp-TDE$_{H10}$ Tumor Culturing: The following procedure has been previous described[41] and was done under a cell-hood. The following mixture is for twelve 1.0 mL Organotypic disks. 11.2×10^6 of BDEsp-TDE$_{H10}$ and 5.6×10^6 of BDEsp-TDF$_{E4}$ cells were diluted into 9.845 mL of 10% DMEM medium. 3.655 mL of filtered Corning® Collagen I, Rat Tail was added to the medium and mixed with a pipette. To induce the solidification of the mixture, 84.1 µL of filtered 1.0 N NaOH solution was added and followed by mixing with a pipette. 1.0 mL of solution was added to each well of a 12-well cell culture plate. The culture was then placed in the cell incubator for 1 to 2 hours, allowing the disk to solidify. Once solidified, the disks were transferred to two 6-well cell culture plates with 3 mL of warm medium. The organotypic culture was placed back into the cell incubator.

2.5.2 3-D Organotypic Treatment, Fixing and embedding: Following was done under a cell-hood. The treatment began the day after organotypic formation. The medium was refreshed before treatment was added. Treatment was refreshed every other day for eight days. After treatment, the organotypic cultures were washed with formaldehyde (37% wt diluted in ddH$_2$O) and then incubated in 5.0 mL of formaldehyde (37% wt diluted in ddH$_2$O) at 8 °C overnight. Samples were then delivered to a histology lab for embedding and sectioning.

26

2.6 Immunohistochemistry.

2.6.1 Paraffin removal, Antigen Unmasking, Blocking: Paraffin-embedded tissue sections on slides are heated at 60 °C for 5 to 10 minutes. The slides are then placed in a cassette and undergo a serious of washes to remove the paraffin and rehydrate the samples. The serious is three 100% xylene submersions for 15 minutes, three 100% ethanol submersions for 10 minutes, 75% ethanol submersions for 5 minutes, 50% ethanol submersions for 5 minutes, 25% ethanol submersions for 5 minutes, and a final wash with ddH$_2$O for 5 minutes. For antigen unmasking, slides were placed in holder filled with 1 mM EDTA buffer pH 8.0 and sub-boiled for 35 minutes. The container and slides were cooled in ice water for 20 minutes. Slides were washed for 5 minutes in ddH$_2$O. To block endogenous peroxidase activity, slides were incubated at RT in 3.0% hydrogen peroxide diluted in methanol for 30 minutes. After blocking, slides are washed with PBST three times for 5 minutes each. Samples were blocked for 1 hour with 0.2% Triton X 100 and 2.5% BSA-PBS blocking solution at RT. This preparation was followed by staining and immunohistochemistry.

2.6.2 Hematoxylin and Eosin: Paraffin removal, antigen unmasking, blocking of samples are described above. Staining was conducted with ABCAM H&E Staining Kit (ab245880). Slides were incubated in hematoxylin for 10 minutes at RT and in the dark. The excess staining was rinsed off with ddH$_2$O for 5 minutes. Excess ddH$_2$O was removed and slides were incubated in Bluing reagent (0.2% Ammonia Water Solution) for 5 minutes at RT. The excess staining was rinsed off with ddH$_2$O for 5 minutes. Slides were incubated in eosin for 15 minutes at RT. The excess staining was rinsed off with ddH$_2$O for 5 minutes. Slides were then washed briefly in 75% ethanol. Samples were then dehydrated with the following serious of washes. Three 100%

ethanol submersions for 10 minutes and three 100% xylene submersions for 15 minutes. Slides were placed flat in a hood for 1 minute to allow air drying. Permount was add on top of the samples and cover slide adhered. The slides were kept in the hood overnight to allow permount to solidify. Stained samples were then sent to MCV Clinical Support Center to be diagnosed.

2.6.3 TROMA-III (CK-19) Staining: Paraffin removal, antigen unmasking, blocking of samples are described above. TROMA-III (CK-19) antibody was purchased from Developmental Studies Hybridoma Bank (DSHB). Samples were incubated in 1:100 TROMA-II antibody diluted in triton X-100 and 2.5% BSA-PBS blocking solution overnight at 8 °C. The primary antibody was then washed off with PBST three times for 5 minutes each. Incubation of secondary antibody and staining was conduct as instructed in rat specific VECTASTAIN® ABC HRP Kit and DAB Peroxidase (HRP) Substrate Kit (with Nickel), 3,3'-diaminobenzidine. Samples are stained with hematoxylin for 20 seconds and rinsed off with ddH$_2$O for 5 minutes. Samples were then dehydrated with the following serious of washes. Three 100% ethanol submersions for 10 minutes each and three 100% xylene submersions for 15 minutes each. Slides were placed flat in a hood for 1 minute to allow air drying. The slides were kept in the hood overnight to allow permount to solidify. The slides were kept in the hood overnight to allow permount to solidify.

2.6.4 Immunofluorescence: Paraffin removal, antigen unmasking, blocking of samples are described above. Samples were incubated in 1:20 primary antibody diluted in triton X-100 and 2.5% BSA-PBS blocking solution overnight at 8 °C. The primary antibody was then washed off with PBST four times for 5 minutes each. Samples were incubated in 1:1,000 secondary antibody diluted in triton X-100 and 2.5% BSA-PBS blocking solution for 1 hour at RT. The secondary antibody was then washed off with PBST four times for 5 minutes each. Excess buffer was

28

removed and cover slips were mounted on the slides with VECTASHIELD® Hardset™ Antifade

Mounting Medium with DAPI (H1500, Vector). Slides were then imaged with confocal

fluorescence microscopy running on ZEISS imaging program.

2.7 CCK-8 Viability Rate.

2.7.1 Treatment and CCK-8 Viability Rate: 4,000 cells were added to each well of a 96-well

plate in 100 µL of 1.0% FBS, warm DMEM medium and placed in cell incubator overnight. 100

µL of fresh 1% FBS, warm DMEM medium containing x2 treatment concentration was added to

each well. The plates were placed in the cell incubator for 48 hours. After incubation, an initial

reading of 450 nm absorbance was conducted on the wells. Three of the wells in the plates were

treated with 10 µL of 1% triton X-100 to act as negative controls. 10 µL of CCK-8 (Cell

Counting Kit-8, Dojindo Laboratories, CK09) was added to each well. Reading of 450 nm

absorbance was conducted between 2 and 4 hours after CCK-8 was added. The survival rate was

then calculated with the initial and final readings. The plates had their initial readings taken at

450 nm to provide a background reading. To create a negative control, in each plate two wells

were treated with 10 µL of 10% triton X-100 and incubated for 15 minutes to allow all the cells

in those well to undergo apoptosis. The cell counting was conducted with a CCK-8 kit. 10 µL of

CCK-8 solution was added to each well and allow to incubate for 2 to 4 hours. Throughout this

time, the plate was periodically read at 450 nm until a few of the readings had a value between

0.9 and 1.0. The final reading was subtracted by initial reading to remove the background for

each well, followed by the negative controls value being subtracted from the background free

final reading to remove the absorbance caused by the natural decay of CCK-8, this would result

in the final value (final value = (final reading – initial reading) - (Negative control – initial

reading)).

2.8 Migration Assay.

2.8.1 Migration Assay: For cell confluency to fall between 70% to 80% confluency in 6-well plates, 0.7×10^6 BDEsp-TDF$_{E4}$ were added to each well in 3 mL of DMEM medium. The cells were placed overnight in cell incubator to allow them to adhere to the plate. A gap was made down the middle of the bed of cells in each well with a 20 µL pipette tip and the medium was refreshed with 1.0% FBS, warm DMEM medium to remove floating cells. Initial imaging of the gap was taken, three images per well. The wells were then treated. Imaging of the same location was done at 24 and 38 hours. The migration rate was then measured with ImageJ.

2.9 Statistics.

Each experiment was repeated at least 3 times ($n \geq 3$). The results are represented as means with SD or SEM error bars. The analysis was performed on GraphPad Prism 8.0 (GraphPad Soft Inc., San Diego, CA). The one-way analysis of variance (ANOVA) and student t-test were used to analyze data and determine statistical significance. Significant P-values were set to $^*P < 0.05$, $^{**}P < 0.01$, $^{***}P < 0.001$, and $^{****}P < 0.0001$.

2.10 Antibodies.

Target Protein	Molecular Weight	Species	Manufacturer	CAT#
SphK1	48 kDa	Rabbit	Santa Cruz	SC-48825
SphK2	69 kDa	Rabbit	ProteinTech	17096-1-AP
S1PR2	50 kDa	Mouse	ProteinTech	21180-1-AP
ERK1/2	44/42 kDa	Rabbit	Santa Cruz	SC-154
p-ERK1/2	44/42 kDa	Mouse	Santa Cruz	SC-7383
Actin	42 kDa	Mouse	DSHB	JLA20
H4K5ac	11 kDa	Rabbit	EpiGentek	A-4027-050
H3K9ac	17 kDa	Rabbit	EpiGentek	A-4022-025
H2BK12ac	15 kDa	Rabbit	EpiGentek	A-68352-050
Histone H3	18 kDa	Rabbit	EpiGentek	A-1112-100

Target Species	Species	Function	Manufacturer	CAT#
Rabbit	Goat	IM	Bio-Rad	170-6515
Mouse	Goat	IM	Bio-Rad	170-6516
Rabbit	Goat	IF	Complete	A21206
Rabbit	Goat	IH	Vector Laboratories	BA-4000

Table 1: Antibodies. A) Antibodies for immunoblotting, target, expected weight, antibody's species of origin, producer, #CAS. **B)** Secondary antibodies and associated procedure. Immunoblotting (IM), immunofluorescence (IF), and immunohistochemistry (IH).

2.11 Nanoparticles.

2.11.1 Nanoparticle Construction and Drug Encapsulation: Nanoparticles were constructed and drug was encapsulated in Dr. Zhu lab, MCV. Five differing nanoparticle subunits were used, each forming their own micelle structure. 2 mg of Nanoparticle subunits were dissolved in 100 µL of tetrahydrofuran. Drug is dissolved into 250 µL of methanol. 50 µL of drug solution is mixed with the nanoparticle subunit solution. The combination mixture was added into 2 mL of ddH₂O and stirred at RT overnight to allow drug encapsulation and organic reagents to evaporate. Solution was centrifuged at 5,000 rpm for 5 minutes to separate the unloaded drug and free polymer. Supernatant was filtered with 0.45 µm filter membrane, resulting in the solution of micelle nanoparticle loaded with drug. (**Table 2**)

Nanoparticles (NP)	Subunit Molecular Structure	Subunits Parts with Molecular Weights
NP1		mPEG$_{5k}$-PLGA$_{5k}$
NP2		mPEG$_{5k}$-PLGA$_{15k}$
NP3		mPEG$_{5k}$-PLGA$_{25k}$
NP4		mPEG$_{5k}$-PCL$_{5k}$
NP5		mPEG$_{5k}$-PLA$_{5k}$
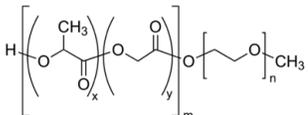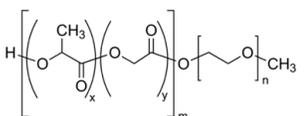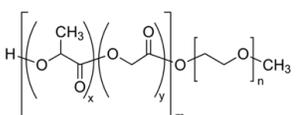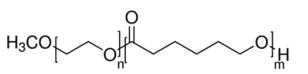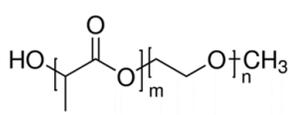
Table 2: Nanoparticle Subunits: Five different nanoparticle micelle structures were used in this study. Each structure was made of one type of nanoparticle subunit. Each subunit shares the mPEG$_{5k}$ base. The displayed monomer structure subunit is repeated to form polymers of various size and attached to the mPEG$_{5k}$ base. The molecular weight (kDa) of the polymer is indicated by the subscript value. The weight and structure of subunit effects its uptake into the cell.

Chapter 3: Rationale and Results

3.0 Rationale and Aim.

The previous studies have found that the S1PR2/SphK2-mediated signaling pathways are linked to CCA cell growth. The overall goal of this study is to determine the effect of inhibiting SphK2 on CCA cell growth.

- Sub Aim 1: Test ABC294640 ability to inhibit CCA and CAFs.
- Sub Aim 2: Determine the mechanical effect of ABC294640 on CCA and CAFs cells.
- Sub Aim 3: Test nanoparticle delivery of ABC294640.

3.1 Effect of SphK2, ABC294640, on CCA and CAF cells.

Previous research has indicated that CCA has increased the expression of S1PR2 and its downstream target, SphK2[27,44]. Inhibiting S1PR2 has proven to inhibit the progression of CCA[27]. This study's focus was determining if inhibiting SphK2 halts the progression of CCA. The primary SphK2 competitive inhibitor chosen for this study is ABC294640, due to its approval for use in clinical trials[37]. ABC294640 dosage assay was conducted on CCA cells, to determine if inhibiting SphK2 activity affects the viability of CCA cells.

Five differing rat CCA cell lines were selected that represented the spectrum of CCA. BDE1 cells are non-tumorigenic immortalized cholangiocytes and act as a negative control. BDEsp-TDE$_{H10}$ is an unmodified CCA cell line. BDEsp-TDE$_{neu}$ and BDEsp-TDE$_c$ are more aggressive forms of CCA. BDEsp-TDE$_{neu}$ possesses a mutation that increased the expression of HER2. BDEsp-TDE$_c$ has an empty vector to act as a control for BDEsp-TDE$_{neu}$. To determine if the treatment affected CAFs cells, BDEsp-TDF$_{E4}$ was included in the dosage assay.

33

The cells were plated in 96-well plates to a confluency of 60% to 80%. The individual plates were treated with various amounts of ABC294640, ranging from 1.0 to 25.0 µM. After 48 hours of treatment incubation, the cell viability for each treatment dosage was measured with CCK-8 as described in the methods. The viability levels were plotted by the relative percentage of survival vs. $\log_{10}$ of ABC294640 dosage. A dosage curve was calculated, revealing the IC_{50} for each cell line (**Figure 10**). The general trend of these results suggests that ABC294640 lethality to a cell line is positively correlated with the malignancy level of the cell line; with BDE1, the least malignant, having the highest IC_{50} of 16.1 µM while BDEsp-TDE$_{neu}$, the most malignant, had the lowest IC_{50} of 9.6 µM, though this is not significant. Interestingly BDEsp-TDE$_{H10}$ had an IC_{50} of 15.1 µM while its CAF partner, BDEsp-TDF$_{E4}$, had an IC_{50} of 14.0 µM; suggesting ABC294640 can also disrupt the cancer microenvironment by inhibiting the CAF cells.

3.2 Viability Measure of CCA and CAF Cells Treated with ABC294640 and/or TCA.

The activation of S1PR2, an upstream activator of SphK2, leads to an increase in the growth of CCA cells[28]. The CBA, Taurocholic acid (TCA), is a ligand of S1PR2 and has been linked to the increased progression of CCA[19]. To determine if ABC294640 can alter the promoting effects of TCA on CCA, a cell viability assay was conducted. To fully represent a CCA tumor, both CCA cells, BDEsp-TDE$_{H10}$, and CAF cells, BDEsp-TDF$_{E4}$, were tested. The two cell types were plated in 96-well plates to a confluency of 60% to 80%. The individual wells were treated with TCA and/or ABC294640. The TCA treatment levels were 25.0, 50.0, and 100 µM. The ABC294640 treatment levels were 12.5 and 25.0 µM. The TCA treatment levels of the two cell types were plated in 96-well plates to a confluency of 60% to 80%. The individual wells

34
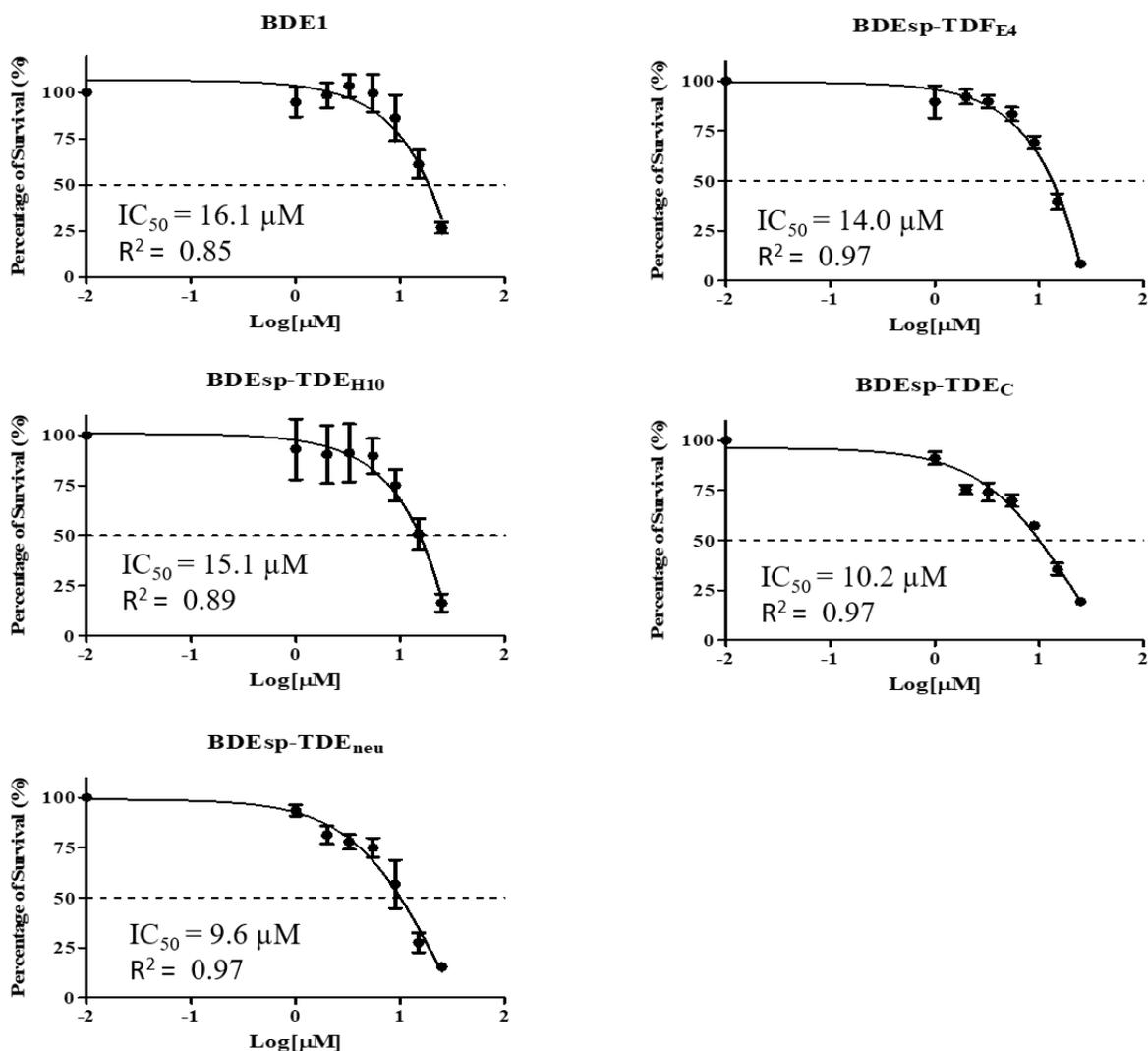
**Figure 10: ABC294640 Dosage Assay of Cholangiocarcinoma Cell lines.** ABC294640 dosage assay of BDE1, BDEsp-TDF$_{H10}$, BDEsp-TDE$_{H10}$, BDEsp-TDE$_{neu}$, and BDEsp-TDE$_{neu}$ cell lines. Survival vs. Log$_{10}$ of ABC294640 concentration dosage curves for varies CCA and CAF cell lines 48 hours after treatment. SD bars, means, IC$_{50}$ values, and R^2 are included. n = 3. Calculations were done on GraphPad prism.

were treated with TCA and/or ABC294640. The TCA treatment levels were 25.0, 50.0, and 100 µM. The ABC294640 treatment levels were 12.5 and 25.0 µM. The TCA treatment levels of 50.0 and 100 µM were paired with both ABC294640 treatment levels. The singular or combination treatments were added to the 96-well plate After 48 hours of treatment incubation, the cell viability for each treatment dosage was measured with CCK-8 as described in the methods. The viability of the various treatment types was compared to control.

The TCA dosage of 50.0 µM significantly ($P^* = 0.0471$) increased the viability of BDEsp-TDE$_{H10}$ cells, while the other TCA dosages did increased viability, but not ($P > 0.05$) significantly. All Treatments including ABC294640 had significantly (12.5 µM, $^*P < 0.05$ and 25.0 µM, $^{***}P < 0.001$) reduced viability. Both TCA dosages (50.0 µM and 100 µM) had significantly ($^{**}P < 0.01$) higher viability than their TCA and ABC294640 cotreatment counterparts. The viability of cells treated with both ABC294640 and TCA was equivalent to cells treated with only ABC294640. This indicates that ABC294640 can completely counter the promoting effect TCA has on CCA. (**Figure 11**)

TCA dosage of 100 µM significantly ($P^* = 0.013$) decreased the viability of BDEsp-TDF$_{E4}$ cells, while the other TCA dosages did decreased viability, but not ($P > 0.05$) significantly. All Treatments including ABC294640 had significantly (12.5 µM, $^{**}P < 0.01$ and 25.0 µM, $^{***}P < 0.001$) reduced viability. TCA dosages (50.0 µM and 100 µM) had significantly ($^*P < 0.05$) higher viability than their TCA and ABC294640 cotreatment counterparts. The viability of cells treated with both ABC294640 and TCA was equivalent to ABC294640 treatment. This data suggests that TCA at high dosages is toxic to BDEsp-TDF$_{E4}$ and that ABC294640 nullifies this toxicity while remaining toxic itself. (**Figure 12**)

36
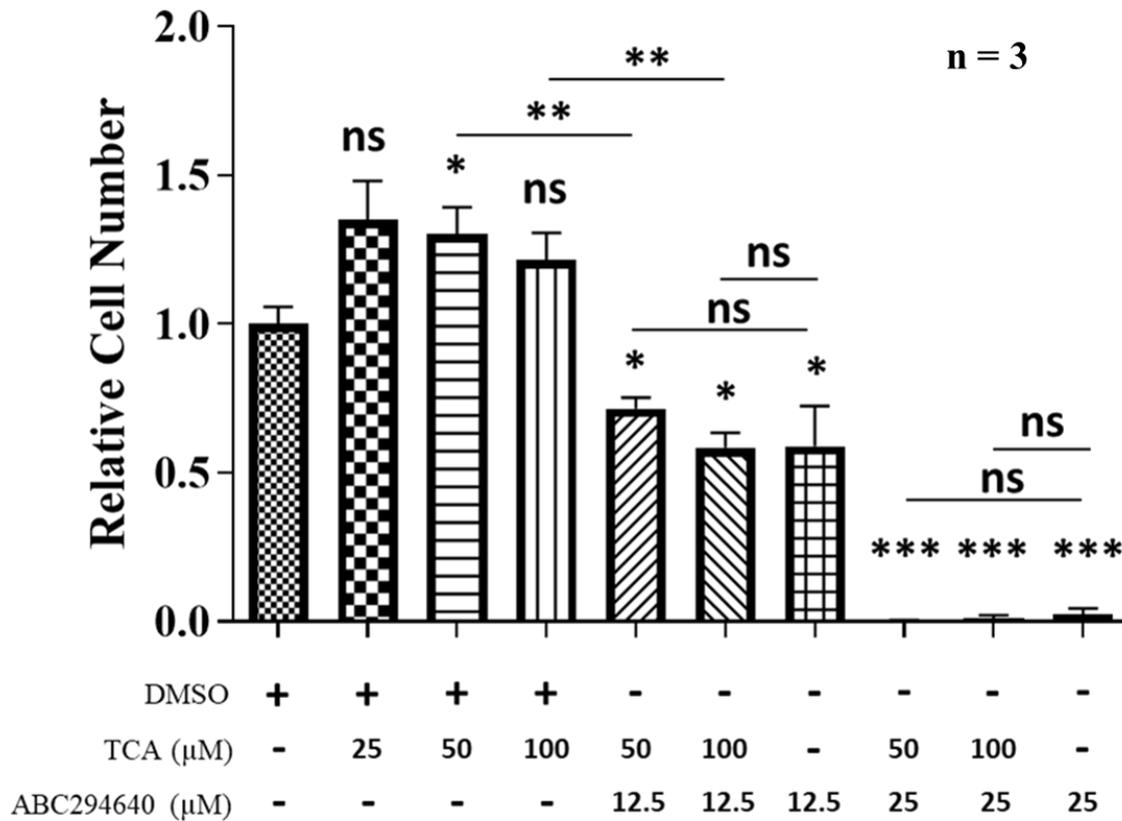
BDEsp-TDE$_{H10}$

Figure 11: **BDEsp-TDE$_{H10}$ Cells Viability Measure with Various Levels of TCA and/or ABC294640.** Cells were plated in 96-well plate, 4,000 per well in 1.0% FBS medium and incubated overnight. Treatment was added and incubated for 48 hours, followed by viability measure with CCK-8. Symbol above bars indicate significant compared to control. n = 3 and values are mean ± SEM. 50 μM TCA significantly (*P = 0.0471) increased viability. ABC294640 reduced cell viability (12.5 μM, *P < 0.05 and 25.0 μM, ***P < 0.001). TCA with ABC294640 were significantly different from their only TCA counterparts (**P < 0.01).

BDEsp-TDF$_{E4}$
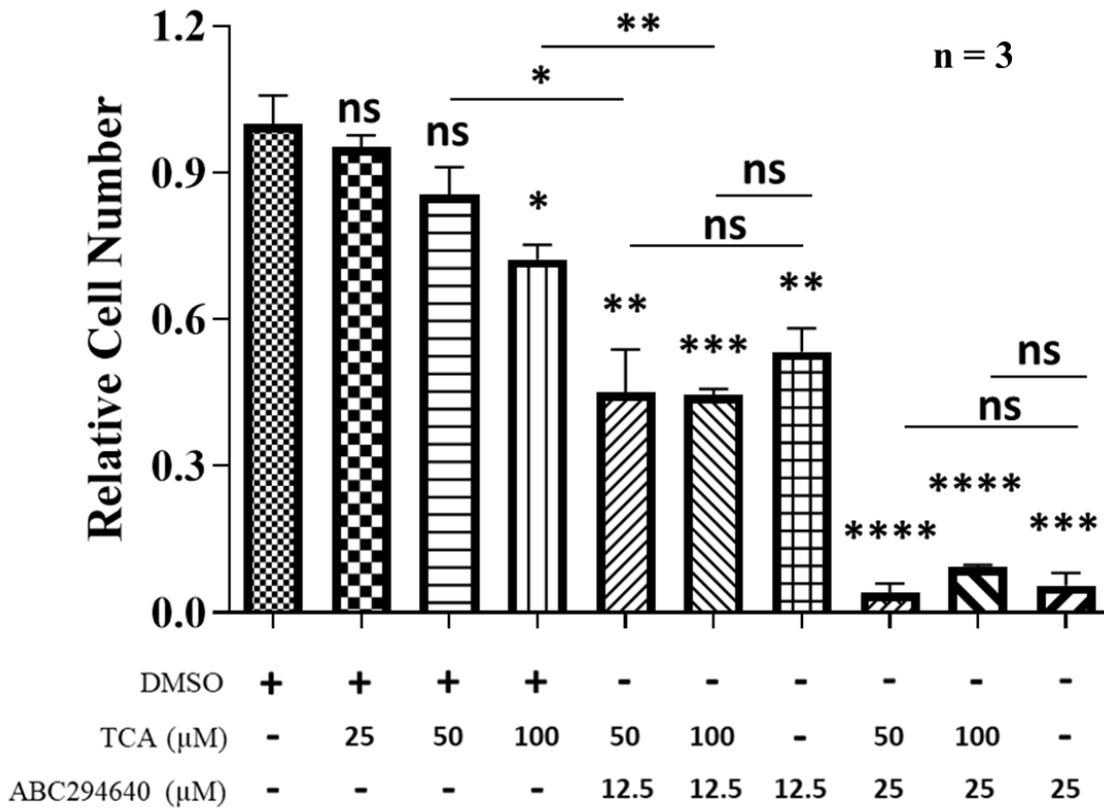
Figure 12: **BDEsp-TDF$_{E4}$ Cells Viability Measure with Various Levels of TCA and/or ABC294640.** Cells were plated in 96-well plate, 4,000 per well in 1.0% FBS medium and incubated overnight.   Treatment was added and incubated for 48 hours, followed by viability measure with CCK-8. Symbol above bars indicate significant compared to control. n = 3 and values are mean ± SEM. 100 µM TCA significantly (*P = 0.013) decreased viability. ABC294640 treatments significantly reduced viability (12.5 µM, **P < 0.01 and 25.0 µM, ***P < 0.001.

3.3 Effect of ABC294640 on Taurocholic Acid-induced Formation of "Duct-Like" Structure in a 3-D Organotypic Culture Model of Rat CCA Cells.

The dosage assay indicated that ABC294640 could disrupt the CCA and CAFs cells in tumors. To determine if ABC294640 could disrupt and inhibit tumor growth, a 3-D Organotypic treatment was performed. The 3-D organotypic culture is a combination of CCA, BDEsp-TDE$_{H10}$, and CAFs, BDEsp-TDF$_{E4}$, cells are suspended in collagen, which forms "duct-like" structures. The creation of this culture has previously been described[43]. The cultures were treated for 8 days with TCA (100 µM) and/or ABC294640 (10 µM). After the treatment period, the cultures were fixed, sectioned, and stained with H&E (**Figure 13A**). The sections were imaged at 10x magnification and the ducts were measured with ImageJ "Analyze Particle" function. The average size (µm^2) of the "duct-like" structures were recorded. The TCA (100 µM) treatment (**P=0.0072) increased the size of the "duct-like" structures. The ABC294640 (10 µM) treatment significantly (****P < 0.0001) decreased the size of the "duct-like" structures. TCA and ABC294640 combination treatment had larger (*P = 0.0281) "duct-like" structure then the ABC294640 treatment, while still having significantly smaller (****P < 0.0001) structures then the TCA treatment group (**Figure 13B**). The count of the "duct-like" structures was recorded. The TCA (100 µM) treatment (**P = 0.009) increased the count of the "duct-like" structures. The ABC294640 (10 µM) treatment significantly (****P < 0.0001) decreased the count of the "duct-like" structures. TCA and ABC294640 combination treatment had fewer (****P < 0.0001) structures then both the control and TCA treatment groups. (**Figure 13C**). The TCA treatment was able to increase the size and amount of "duct-like" structures, indicating that activation of the S1PR2/SphK2 pathway does promote the growth of the simulated tumors. The inhibition of SphK2 by ABC294640 decreased the size and amount of the "duct-like", as
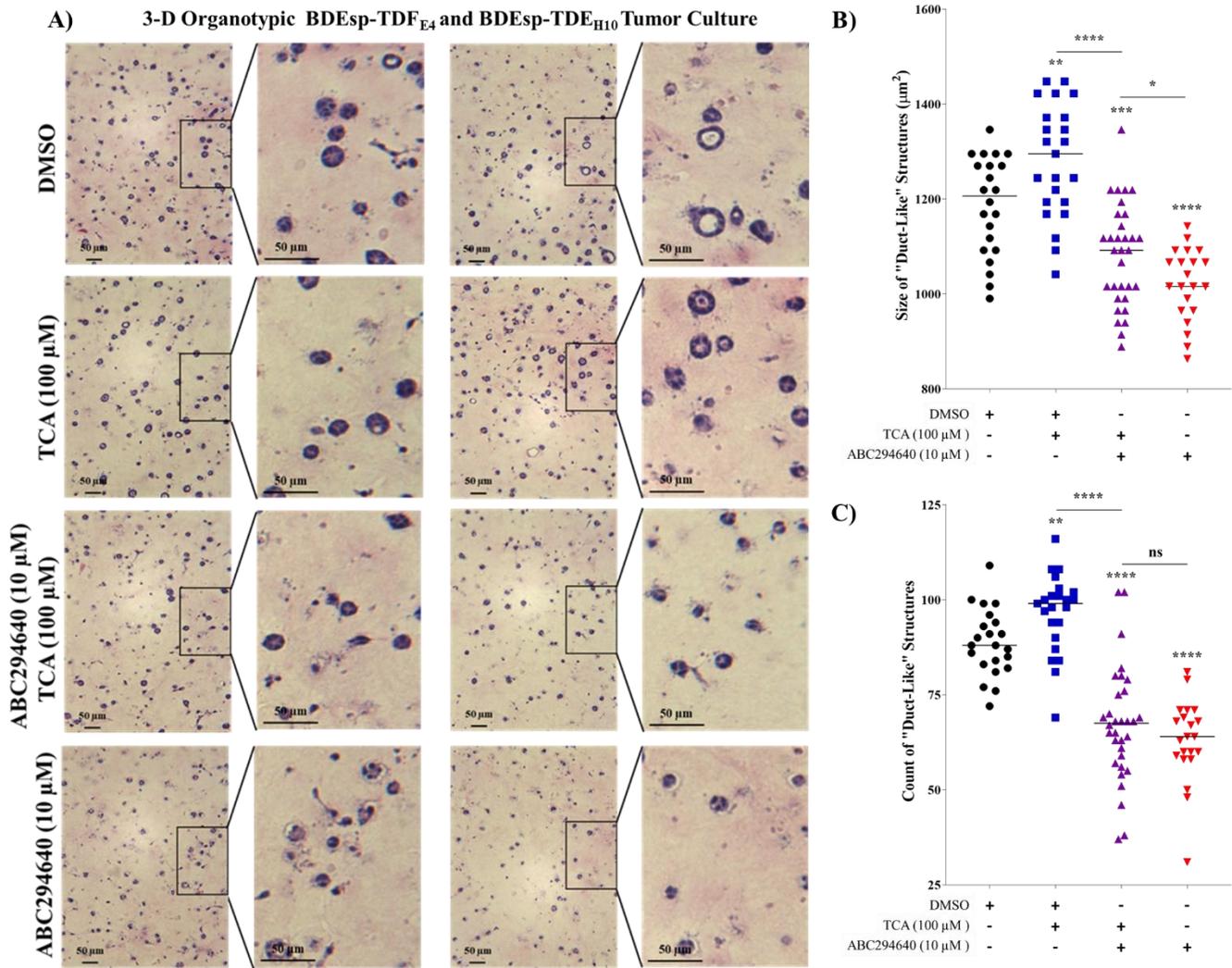
Figure 13: **3-D Organotypic Co-Culture.** TCA and ABC294640 Treatment of BDEsp-TDE$_{H10}$ and BDEsp-TDF$_{E4}$ Cells 3-D Organotypic Co-culture. Rat BDEsp-TDE$_{H10}$ and BDEsp-TDF$_{E4}$ co-culture were solidified together in rat tail type-1-collagen gel disk. The co-culture disk was incubated for 8 days with 100 µM TCA and/or 10 µM ABC294640 treatments. The co-culture was fixed and sectioned. The section was stained with H&E. Images were taken of the "duct-like" structures in each sample. Duct size and count was quantified with ImageJ. Symbol above bars indicate significant compared to control. Line indicates mean. n = 9. (A) Representative image of H&E stained spheroid/"duct-like" structures for each treatment. (B) The average size (µm^2) of "duct-like" structures per image. TCA treatment did (**P=0.0072) increase the size of "duct-like" structures. Both groups treated with ABC294640 had significantly (****P < 0.0001) reduced size, while the combination treated group had larger (*P = 0.0281) structures compared to the ABC294640 treatment group. TCA treatment and TCA with ABC294640 were significantly (****P < 0.0001) different. (C) Count of "duct-like" structure per image. 100 µM TCA had a significant ((**P = 0.009) increased count. Both groups treated with ABC294640 had significantly (****P < 0.0001) reduced count and had equivalent counts. TCA treatment and TCA with ABC294640 were significantly (****P < 0.0001) different.

expected. The ABC294640 and TCA combination treatment had equivalent "duct-like" structure count compared to ABC294640 treatment, which indicates that ABC294640 treatment could be halting the tumor's ability to metastasize and migrate to another portion of the culture. These results agree with a study that conducted the same experiment with S1PR2 inhibitor treatment[28].

3.4 Cell Migration Assay.

CCA tumor's metastasis and infiltration capability are largely dependent on the CAFs cells, which detaches from the surrounding tissue allowing the tumor to metastasize and are at the front of tumor migration. To determine if ABC294640 can inhibit CAFs role in cancer metastasis, a migration assay was conducted. The protocol of the migration assay is described in the methods. The cells were treated with TCA (100 µM) and/or ABC294640 (12.5 or 25 µM). The images were taken immediately before treatment and 36 hours after treatment. TCA (100 µM) increased (****$P < 0.0001$) the migration rate of BDEsp-TDF$_{E4}$. ABC294640 decreased (**$P < 0.002$) the migration rate of BDEsp-TDF$_{E4}$ cells. Interestingly, 12.5 µM ABC294640 treatment with and without TCA were equivalent. This could indicate that even at a low dosage, ABC294640 can block the effects of TCA. The 25 µM ABC294640 dosage was very effective (****$P < 0.0001$) at inhibiting migration, though TCA was able to counter this slightly (**$P = 0.0026$). (**Figure 14**)

The same migration assay was conducted with BDEsp-TDE$_{H10}$ cells with the same procedure. The final images were taken at 24 hours after treatment, due to BDEsp-TDE$_{H10}$ higher migration rate. The TCA treatment increased (*$P = 0.0217$) the migration rate of the BDEsp-TDE$_{H10}$ cells, but not as significant (****$P < 0.0001$) as the BDEsp-TDF$_{E4}$ cells. 12.5 µM ABC294640 treatment reduced (**$P = 0.001$) the migration rate of BDEsp-TDE$_{H10}$. The 25 µM

41

ABC294640 treatment was able to significantly reduce the migration rate (**P < 0.005) of BDEsp-TDE$_{H10}$. (**Figure 15**)

The migration rate is increased by TCA (100 µM) treatment and decreased by ABC294640 treatment in both BDEsp-TDE$_{H10}$ and BDEsp-TDF$_{E4}$ cell lines. The low dosage of ABC294640 (12.5 µM) can counter TCA treatment. (**Figures 14** and **15**)

3.5 Nanoparticle Delivery of SphK2 Inhibitor.

Nanoparticle constructs can improve the transport of SphK2 inhibitor molecules to CCA cells, by removing the difficulty the hydrophobic molecules have moving through the plasma/lymph. We partnered with Dr. Zhu lab to develop and test nanoparticle's ability to deliver SphK2 inhibitors to CCA, BDEsp-TDE$_{H10}$, cells and their associated CAFs, BDEsp-TDF$_{E4}$. Five nanoparticle constructs were developed and implanted with the inhibitors, ABC294640 and K145.

The two cell types were plated in 96-well plates to a confluency of 60% to 80%. The individual wells were treated with SphK2 inhibitor (ABC294640 and K145) within or without the nanoparticle construct. The ABC294640 treatment dosages were 12.5 and 25 µM. The K145 treatment dosages were 5.0 µM and 10 µM. These dosages seem to be less effective than previous dosage assay, possibly due to the nanoparticle encapsulation process degrading the drug. The free drug went through the same process and still acts as an effective positive control. Treatments were added to corresponding wells of 96-well plate. After 48 hours of treatment incubation, the cell viability was measured with CCK-8 as described in the methods. The final viability of each treatment type was compared with control.

42
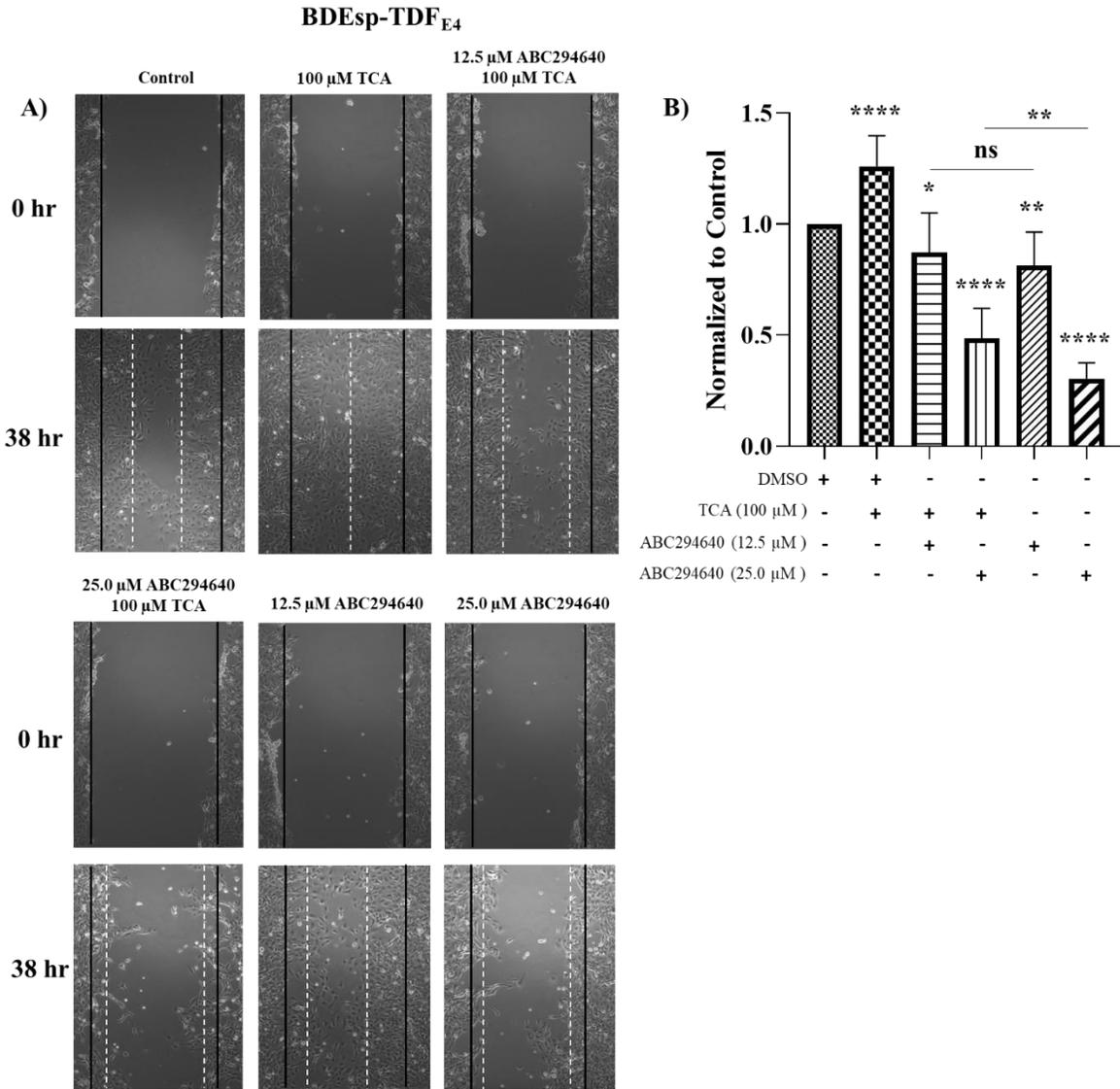
Figure 14: BDEsp-TDF$_{E4}$ Migration Assay with TCA (100 µM) and/or ABC294640 (12.5 and 25 µM) Treatments. Cells were plated to 70% - 80% confluency in 6-well plate with 10% FBS medium. A wound was scratched down the middle of the plate and the medium was placed with 1.0% FBS medium. Images were taken at 4x magnification. Initial images were taken and treatment was added. Final image was taken at 24 hours. (A) Initial and final images of scratch assay of various treatments. Experiment was replicated 3 times and each well had imaging 3 spots, n = 9. Values are mean ± SEM. (B) Distant of migration normalized to control. TCA increased (****$P < 0.0001$) migration rate. 12.5 µM ABC294640 with TCA treatment did have significant (*$P = 0.0481$) decrease in migration and 12.5 µM ABC294640 treatment did see a decrease (**$P = 0.002$) in migration. Both treatments with 25 µM ABC294640 had significant (**$P < 0.0001$) decrease in migration. Both TCA and 12.5 µM ABC294640 combination treatments were equivalent to their 12.5 µM ABC294640 treatment counterpart, while TCA and 25 µM ABC294640 treatment had increased (**$P = 0.0026$) migration compared to 25 µM ABC294640.
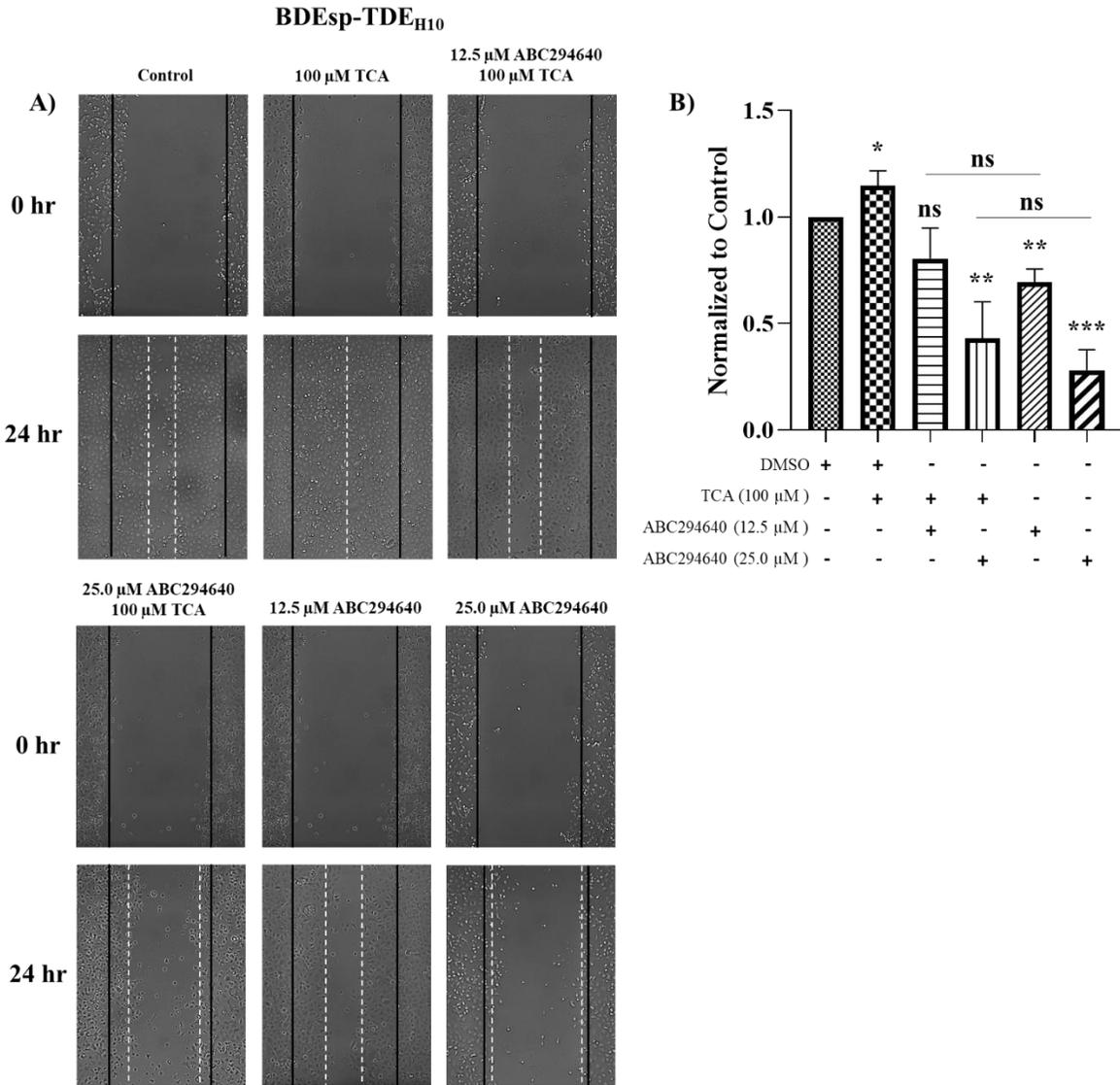
Figure 15: **BDEsp-TDE$_{H10}$ Migration Assay with TCA (100 μM) and/or ABC294640 (12.5 and 25 μM) Treatments.** Cells were plated to 70% - 80% confluency in 6-well plate with 10% FBS medium. A wound was scratched down the middle of the plate and the medium was placed with 01% FBS medium. Images were taken at 4x magnification. Initial images were taken and treatment was added. Final image was taken at 36 hours. (A) Initial and final images of scratch assay of various treatments. (B) Distant of migration normalized to control. Experiment was replicated 3 times and each well had imaging 3 spots, n = 9. TCA increased (*P = 0.0217) migration rate. 12.5 μM ABC294640 with TCA treatment did not have significant decrease in migration, while 12.5 μM ABC294640 treatment did see a decrease (**P = 0.001) in migration. Both treatments with 25 μM ABC294640 had significant (**P < 0.005) decrease in migration. Both TCA and ABC294640 combination treatments were equivalent to their ABC294640 treatment counterpart.
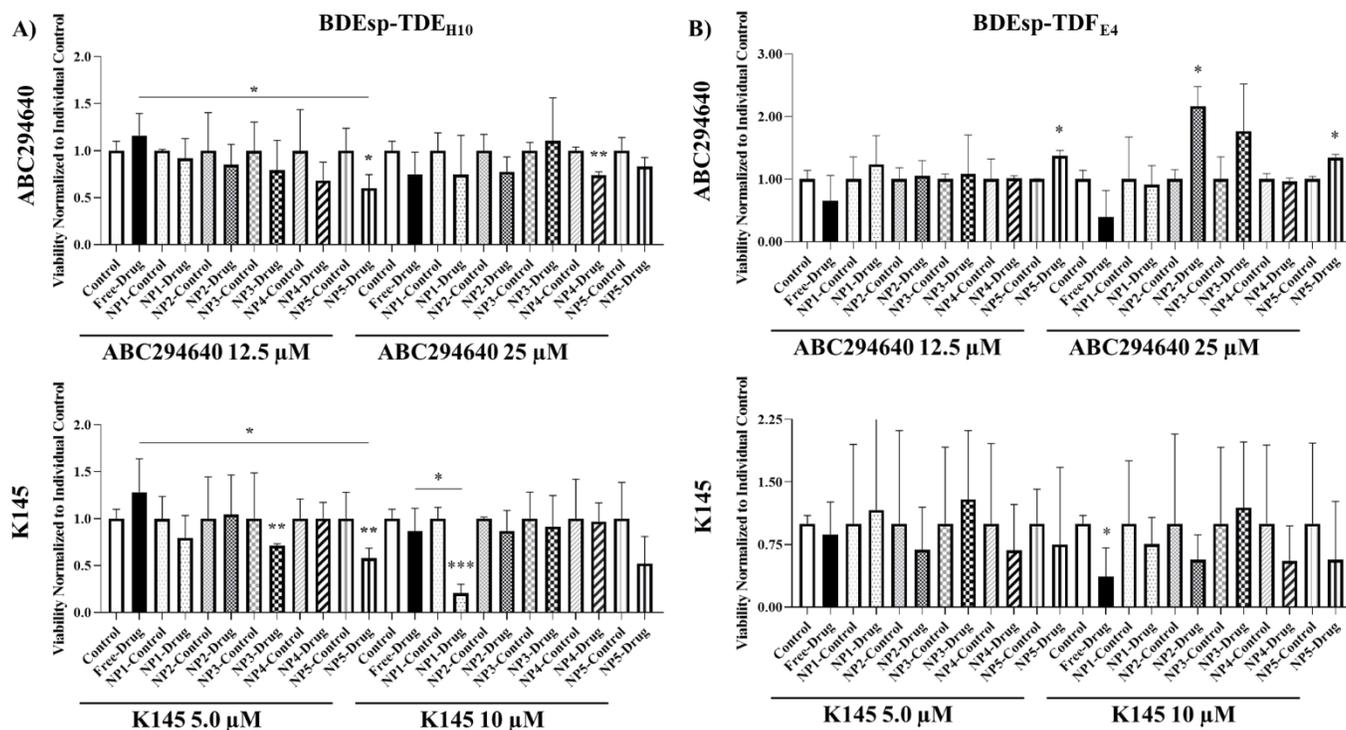
Figure 16: Nanoparticle Delivery of SphK2 Inhibitors Viability Assay. The treatments were delivered in free form or in one of the 5 design nanoparticle constructs. The ABC294640 treatment dosages were 12.5 µM and 25 µM. The K145 treatment dosages were 5.0 µM and 10 µM. n = 3 and values are mean ± SEM. A) The viability measure of BDEsp-TDE$_{H10}$. B) The viability measure in BDEsp-TDF$_{E4}$.

In the BDEsp-TDE$_{H10}$ cells, nanoparticle type 5 was the most effective in both drug types. In BDEsp-TDF$_{E4}$, none of the nanoparticles were effective. More research and development need to be conducted. (**Figure 16**)

3.6 Effect of SphK2 inhibitor on Histone Acetylation in rat CCA and CAFs cells.

As described before (**Figure 6**), TCA can induce acetylation via the S1PR2/SphK2 pathway. To determine if this pathway is maintained in CCA (BDEsp-TDE$_{H10}$) and CAFs (BDEsp-TDF$_{E4}$), cells were treated with TCA, and acetylated histone levels were measured with immunoblotting. Cells were plated to 70% to 80% confluency. The cells medium was refreshed with 1.0% FBS medium and allowed to incubate for 1 hour. The TCA dosages of 0, 50, 100, and 200 µM were added to the plates and allowed to incubate for 4 hours in a cell incubator. Once incubation completed, the nuclear protein was extracted. Immunoblotting for H4K5, H2BK12, H3K9, and H3 as an internal standard was performed as described in the methods. In BDEsp-TDE$_{H10}$ the TCA treatments of 50 µM (*$P < 0.05$) and 100 µM (**$P < 0.01$) increased acetylation consistently across the various histones. In BDEsp-TDF$_{E4}$ the TCA treatments did not increase histone acetylation. The TCA (200 µM) treatment did decrease (**$P < 0.01$) the acetylation of H3K9. This data suggests that the BDEsp-TDE$_{H10}$ cells are being affected by TCA treatment via the S1PR2/SphK2 pathway, while the BDEsp-TDF$_{E4}$ is being affected in a different way or on a different time scale (**Figure 17**). TCA treatment is inducing histone acetylation in BDEsp-TDE$_{H10}$ cells, ABC294640 could possibly affect this increased acetylation. The same procedure for preparing and treating the cells was followed, except that BDEsp-TDE$_{H10}$ cells were treated with TCA (100 µM) and/or ABC294640 (25 µM). 4 hours after treatment, the nuclear protein was extracted. Immunoblotting for H4K5, H3K9, and H3 as an internal standard was performed as described in the methods. the nuclear protein was extracted.
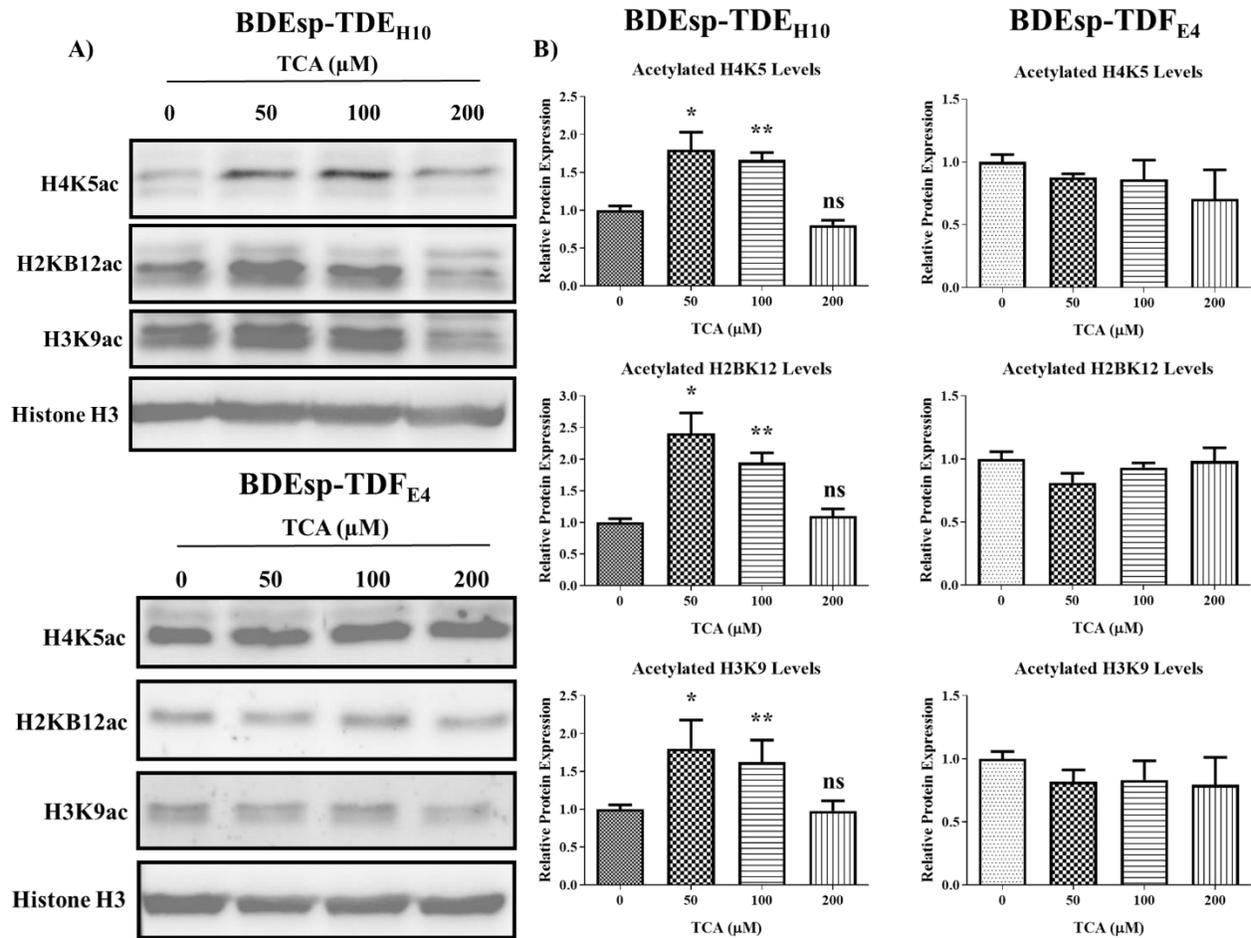
Figure 17: TCA Effect on Histone Acetylation. Protein was collected from BDEsp-TDE$_{H10}$ and BDEsp-TDF$_{E4}$ cell lines treated with various TCA levels for 4 hours, followed by nuclear protein extraction as described in the methods and stored at -80 °C. Protein levels of H4K5, H2KB12, H3K9, and H3 (standard) were determined by immunoblotting analysis. (A) Representative images of immunoblotting of cell treated with various levels of TCA treatments. Statistical: n = 3 and values are mean ± SEM. Student t-test was used to determine if protein levels were significant between treatments. (B) Quantification of average protein levels for the four treatments. In BDEsp-TDE$_{H10}$ the 50 μM (*P < 0.05) and 100 μM (**P < 0.01) of TCA treatment increased acetylation constantly across all type of histones. In BDEsp-TDF$_{E4}$ the TCA treatments did not increase histone acetylation. The 200 μM treatment did decrease (**P < 0.01) the acetylation of H3K9.

Immunoblotting for H4K5, H3K9, and H3 as an internal standard was performed as described in the methods. H2KB12 was not repeated due to a lack of antibodies. The treatments changed the acetylation levels of histones in BDEsp-TDE$_{H10}$. For H4K5 and H3K9, TCA (100 µM) increased (*P < 0.05) acetylation, TCA (100 µM) with ABC294640 (25 µM) decreased (*P < 0.05) acetylation, and ABC294640 (25 µM) treatment's histone acetylation level was equivalent to the control. The difference of acetylation is significant (**P < 0.01) between TCA (100 µM) with or without ABC294640 (25 µM). There was no significant difference between ABC294640 (25 µM) treatments with or without TCA (100 µM). ABC294640 is halting the acetylation induced by TCA treatment, yet doesn't reliably decrease acetylation by itself. This makes ABC294640 a more promising CCA treatment if the drug specifically targets cells with highly active SphK2. (**Figure 17**)

3.7 Hematoxylin and Eosin Staining of Human Samples.

To determine if the CCA patients had liver maladies, samples were assessed by a histologist. The sample slides were stained with hematoxylin and eosin (H&E) and sent for evaluation. The CCA patient samples had signs of various liver malformations and damage. This includes steatosis, Cirrhosis, fibrosis, mild cholestasis, ductal proliferation, and polymorphous infiltrate. These results confirm that CCA patients' livers were undergoing stress associated with CCA (**Figure 19**).

3.8 TROMA-III (CK-19) Staining of Human Samples.

CK-19 is a marker for fibrosis and for cancer infiltration. CCA patient's samples were probed for CK-19, followed by immunohistochemistry staining. CCA patients had a slight
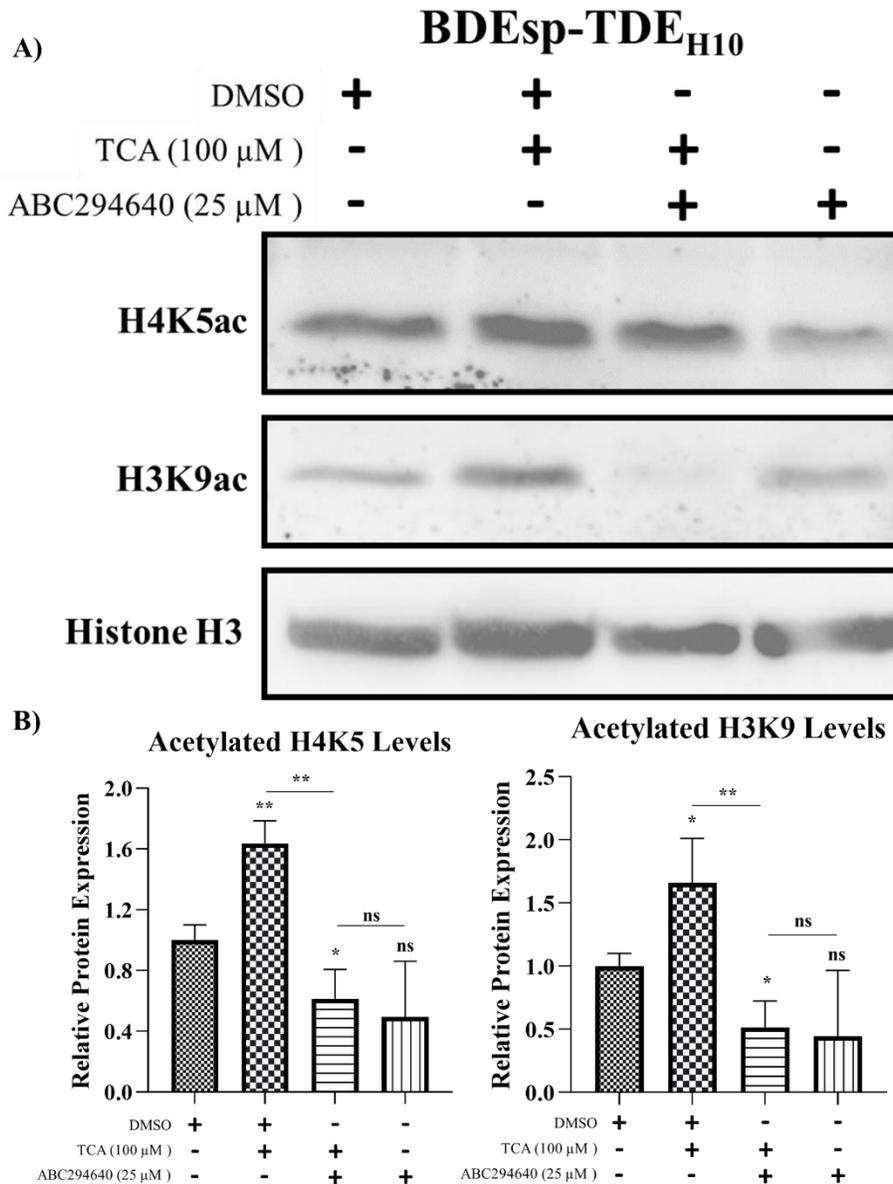
Figure 18: **Effect of TCA and/or ABC294640 Treatment of Histone Acetylation in CCA Cells.** Protein was collected from BDEsp-TDE$_{H10}$ cell lines treated with various TCA (100 μM) and/or ABC294640 (25 μM) for 4 hours, followed by nuclear protein extraction as described in the methods and stored at -80 °C. Protein levels of H4K5, H2KB12, H3K9, and H3 (standard) were determined by immunoblotting analysis. (A) Representative images of immunoblotting of cell of TCA and/or ABC294640 treatments. (B) Quantification of average protein levels for the four treatments. Statistical significance: n = 3 and values are mean ± SEM. Student t-test was used to determine if protein levels were significant between treatments. For both H4K5 and H3K9, TCA (100 μM) has increased (H4K5: **P = 0.0035, H3K9: *P = 0.0358) acetylation, TCA (100 μM) with ABC294640 (25 μM) has decreased (H4K5: *P = 0.0373, H3K9: **P = 0.0225) acetylation, and ABC294640 (25 μM) doesn't have a change in acetylation. The difference of acetylation is significant (H4K5: **P = 0.0019, H3K9: **P = 0.0085) between TCA (100 μM) with or without ABC294640 (25 μM). There was no significant difference between ABC294640 (25 μM) treatments with or without TCA (100 μM).

Figure 19: **H&E staining of liver sections originated from CCA patients or patients that passed away due to brain trauma (Controls).** Samples were stained with H&E and analyzed by a histologist. Images of 4x and 10x magnification accompanied by histologist diagnosis of sample. CCA patient samples had various signs of liver disease that is linked to CCA. These includes steatosis, Cirrhosis, fibrosis, mild cholestasis, ductal proliferation, and polymorphous infiltrate.
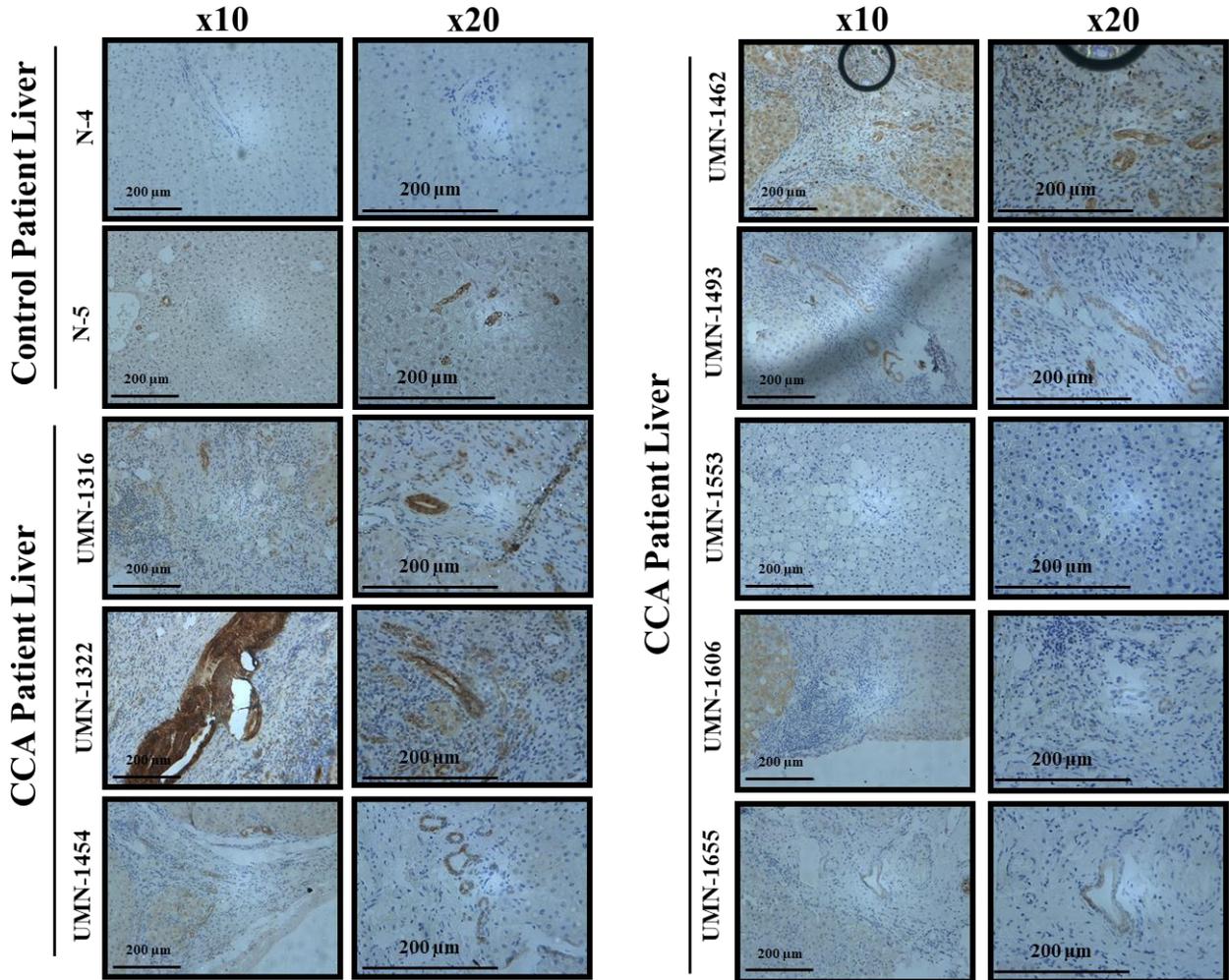
Figure 20: Immunohistochemistry TROMA-III (CK-19) staining of liver sections originated from CCA patients or patients that passed away due to brain trauma (Controls). TROMA-III (CK-19) is a marker for fibrosis. Samples were probed with TROMA-III (CK-19) followed by immunohistochemistry staining. CCA patient liver samples had slightly increased levels of CK-19.

increase in CK-19 expression compared to control, but not significantly. This collaborates with the histologist's conclusion on the H&E stained samples (**Figure 20**).

3.9 Quantifying Protein Expression of Human Liver Samples.

Protein levels of S1PR2, SphK2, and SphK1 in CCA patients were measured. Total protein lysate was collected from CCA patients and control patients (head trauma) liver samples. Three portions from different parts of the liver were collected for each sample. The protein samples were collected and immunoblot as described in the methods. The CCA patient samples have increased levels of S1PR2 (**$P = 0.0033$) compared to the control. This paired with the increased (*$P = 0.0497$) levels of SphK2 indicates the S1PR2/SphK2 pathway is upregulated in CCA patient liver. A slight increase in SphK1 was detected which can contribute to the activation of the S1PR2 via S1P.

3.10 Sphingosine Kinase 2 and Sphingosine-1-Phosphate Receptor 2 Immunofluorescence Histochemistry of Human Samples.

To support the protein quantification results of the human samples, immunofluorescence histochemistry of SphK2 and S1PR2 was conducted. The sample slides were prepared as described in the methods and probed for SphK2 and S1PR2. The samples tested positive for both probed proteins and it appears that the CCA samples possessed higher levels of both proteins (**Figure 22**).
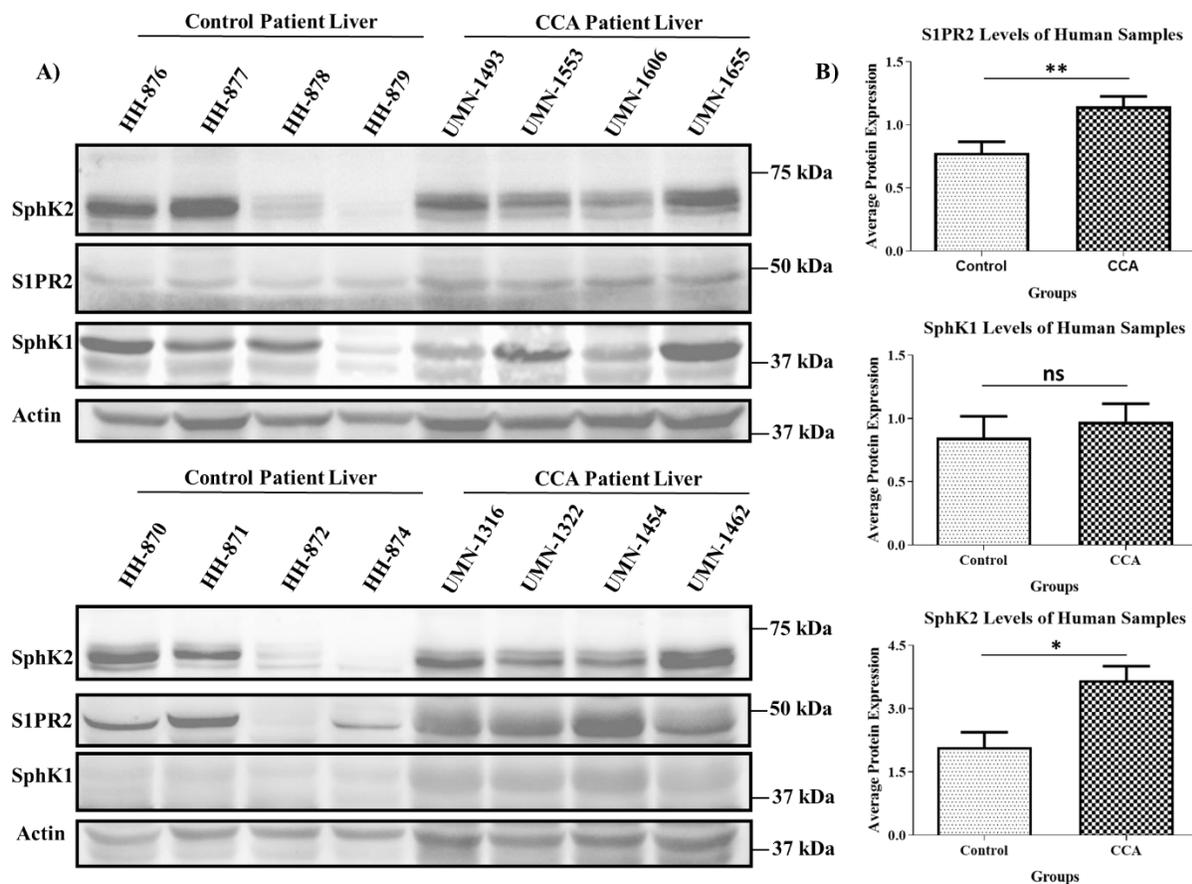
Figure 21: Immunoblotting of Human Samples. Protein was collected from human liver samples the originated from CCA patients or patients that passed away due to brain trauma (Controls). 50 mg of liver tissue was homogenized in 1.0 mL of total protein lysis buffer and stored at -80 °C. Protein levels of SphK2, S1PR2, SphK1, and Actin (standard) were determined by immunoblotting analysis. Statists: 3 liver section from each 8 samples from each group, n = 24. Values are mean ± SEM. Student t-test was used to determine if protein levels were significant between groups. (A) Representative images of immunoblotting for individual patient samples. (B) Quantification of average protein levels for the two groups. S1PR2 (**P = 0.0033) was significant, SphK1 (P = 0. 5697) was insignificant, and SphK2 (*P = 0.0497) was significant.
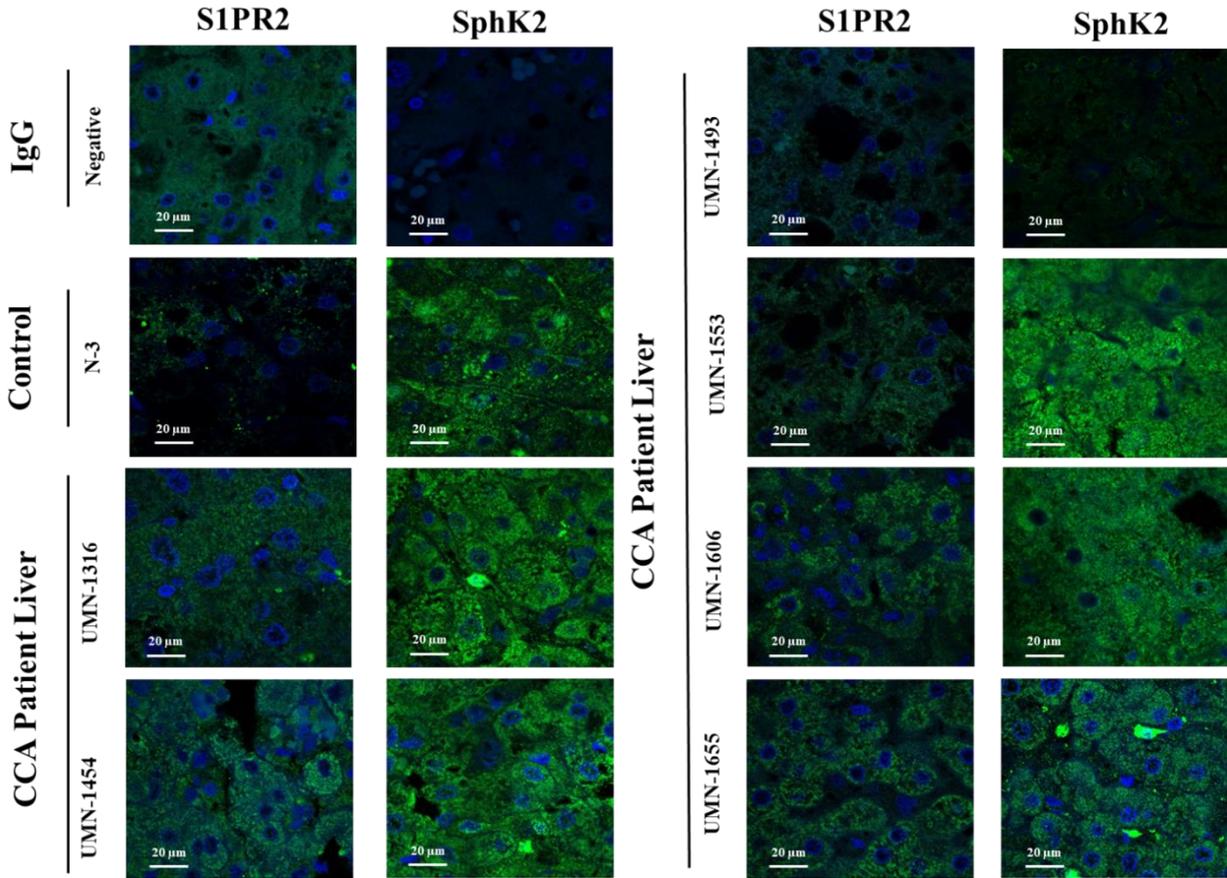
Figure 22: Immunofluorescence Imaging of Patient Samples. Immunofluorescence probing of liver sections originated from CCA patients or patients that passed away due to brain trauma (Controls). Samples were probed for SphK2 or S1PR2, followed by DAPI staining. Images were taken with a fluorescence confocal microscope. IgG negative control Included. It appears that the CCA samples contained higher levels of SphK2 and S1PR2.

Chapter 4: Discussion

Cholangiocarcinoma (CCA) diagnosis rate has been increasing, especially outside the regions it is traditionally found[1]. 20% of CCA cases are identified at the early stage of the disease, this allows for early treatment giving the patient a 30% to surviving 5-year past diagnosis. Patients diagnosed at the late stages of CCA have ~2% of survival over the same time period, even with treatment[2, 43]. The increasing rate of CCA in the global population and the ineffectiveness of treatment at the early and late stages of the disease have created a growing need for novel CCA treatments. Current research indicates that the activation of sphingosine-1-phosphate-receptor-2 (S1PR2) promotes the progression of CCA, possibly through sphingosine kinase 2 (SphK2)[27]. S1PR2 activation leads to the activation of SphK2 in the nucleus, where SphK2 indirectly deactivates HDAC1/2 leading to increased histone acetylation and alteration of gene expression[26]. This epigenetic effect could be the reason for SphK2 activity being associated with cancer neoplastic transformation, tumorigenesis, migration, proliferation, metastasis, metabolism, drug resistance, and overall cancer progression[27, 44 - 46]. SphK2 links to cancer progression make it a prime target for treatment.

Recently ABC294640, an SphK2 competitive inhibitor, has been approved for the clinical trial at 250 mg oral daily dosage (~ 7 µM)[36,47]. In phase I clinical study with a panel of patients with different cancers, a patient suffering from metastatic CCA was given a daily regimen of 250 mg ABC294640 treatment. This CCA patient had the best outcome out of the study, which is encouraging and anecdotal[47]. ABC294640 ability to treat CCA is not well understood. This study examined if ABC294640 can halt or reverse the progression of CCA and the underlining mechanism of this effect.

This study employed various rat CCA, CAF, and cholangiocytes cell lines. To ensure that the ABC294640 treatment could effectively inhibit CCA progression at a reasonable dosage, a dosage assay was done on the panel of CCA cell types. The cells least affected by the treatment were the healthy cholangiocytes, BDE1, with an IC_{50} of 16.1 µM, which suggests that ABC294640 treatment is less toxic to healthy cells compared to the cancer cell lines, though this is speculative. The CCA cell lines BDEsp-TDE$_{H10}$, BDEsp-TDE$_C$, and BDEsp-TDE$_{neu}$ had IC_{50} of 15.1 µM, 10.2 µM, and 9.6 µM respectively (**Figure 10**). A recent study on human intrahepatic CCA cell lines found ABC294640 treatment reduced the viability in the human CCA cell lines[47], indicating ABC294640 can be an effective treatment for targeting patient's CCA cells. Interestingly, cancer-associated myofibroblasts (CAFs) cell line, BDEsp-TDF$_{E4}$, had a similar IC_{50}, 14 µM, to the CCA cell lines (**Figure 10**). CAFs are important for the development of the cancer microenvironment as the CCA cell themselves[29], thus ABC294640 is capable of inhibiting CAFs bolster its use as a CCA treatment. Since all the CCA cell lines had similar responses, we decided to focus on BDEsp-TDE$_{H10}$ representing CCA and BDEsp-TDF$_{E4}$ representing CAFs.

S1PR2 activation of SphK2 is necessary for SphK2 rule in CCA progression[27]. To determine if the S1PR2 pathway was intact and if the pathway could be blocked by ABC294640, a viability assay of BDEsp-TDF$_{E4}$ and BDEsp-TDE$_{H10}$ was conducted. The CBA ligand, taurocholic acid (TCA), was used to activate S1PR2 pathway. Surprisingly the TCA (100 µM) treatment reduced the viability of CAFs, BDEsp-TDF$_{E4}$, but the ABC294640 treatments continued to reduce the cell viability with or without the presence of TCA (**Figure 12**). More predictively, the CCA cells, BDEsp-TDE$_{H10}$, viability was increased be the TCA treatments. The ABC294640 treatments were able to completely counter the effects of TCA, with cells treated

56

with ABC294640 and TCA having equivalent viability to cells treated with only ABC294640 (**Figure 11**). This suggests that the ABC294640 can completely block the TCA ability, via S1PR2/SphK2 pathway, to increase cell viability.

After determining ABC294640 can effectively inhibit the CCA and CAFs that compose CCA tumors, treatment of the simulated tumor was conducted. The 3-D organotypic culture was made with BDEsp-TDF$_{E4}$ and BDEsp-TDE$_{H10}$, which together form "duct-like" structures that are a simulation of CCA tumors. The cultures were treated with TCA to promote and/or ABC294640 to inhibit the progression of the simulated CCA tumors. TCA treatment increased the size and number of the "duct-like" structures, indicating that promoting the S1PR2 pathway quickens the growth and possibly metastasis of the CCA. ABC294640 treatment did the opposite even in the cotreatment with TCA (**Figure 13**). This indicates that ABC294640 can stop tumor growth and metastasis even when the activity of S1PR2 and SphK2 is increased. This outcome is supported by a study that had a similar result with S1PR2 inhibitor instead of an SphK2 inhibitor[27].

To conform ABC294640 ability to halt CCA migration/metastasis, a migration assay was conducted with BDEsp-TDF$_{E4}$ and BDEsp-TDE$_{H10}$. The migration assay was done with TCA and/or ABC294640 treatments (**Figures 14** and **15**). In both cell lines, TCA significantly increased and ABC294640 decreased migration, supporting ABC294640 ability to inhibit CCA metastasis. ABC294640 ability to inhibit CAFs, BDEsp-TDF$_{E4}$, migration rate is important, due to CAFs rule of spearheading migration for the CCA tumors[29].

It was previously discussed that SphK2 indirectly increases the level of histone acetylation[26]. To determine if this pathway was present in BDEsp-TDF$_{E4}$ and BDEsp-TDE$_{H10}$ cell lines, the cells were treated with various levels of TCA and then the histone acetylation

levels were measured with immunoblotting. In CCA, BDEsp-TDE$_{H10}$, the 50 and 100 µM TCA treatments increased histone acetylation. The CAFs, BDEsp-TDF$_{E4}$, histone acetylation decreased after TCA treatment, but this was only significant with H3K9 at 200 µM dosage (**Figure 17**). The S1PR2/SphK2/HDAC1/2 pathway is functional in the BDEsp-TDE$_{H10}$ cell line, allowing it to be a modal to determine if ABC294640 treatment could affect histone acetylation. The same experiment was repeated on BDEsp-TDE$_{H10}$ with TCA (100 µM) and/or ABC294640 (25 µM) treatments. The TCA treatment maintained its ability to increase histone acetylation. More interestingly is ABC294640 didn't reliably decrease acetylation by itself, but when paired with TCA the histone acetylation levels significantly dropped (**Figure 18**). This can indicate that ABC294640's ability to decrease histone acetylation is only effective when SphK2 activity is increased by S1PR2 and not when Sphk2 is at basal activity levels.

The ABC294640 seems to be effective at halting the S1PR2/SphK2 pathway in the CCA cell model. More evidence needs to be present to support ABC294640 as a possible clinical treatment for CCA. To confirm if ABC294640 target pathway was significantly present in patients diagnosed with CCA, SphK2 and S1PR2 quantification was conducted on patient liver samples. The liver disease state of the patients was confirmed with H&E and CK-19 staining of the sample slides, which both showed the patients had various signs of liver disease (**Figures 19** and **20**). The SphK2 and S1PR2 levels were measured with immunoblotting and immunofluorescence, both methods conforming an increase in SphK2 and S1PR2 in CCA patients compared to controls (**Figure 21** and **22**). The increased expression of SphK2 and S1PR2 in CCA patient samples supports the singular phase I clinical study that indicated ABC294640 as an effective treatment for CCA[47].

Based on this study, ABC294640 shows great promise as a CCA treatment for the following reasons. The drug has higher toxicity to CCA cell lines compared to the healthy cholangiocyte cell line. The inhibiting effects were also effective on CAFs, which are important for CCA progression. The treatment stopped the metastasis and growth of tumors, even in the presence of the CCA promoter, TCA. The drug's mechanical effect of stopping histone acetylation may only affect cells with highly active SphK2, which makes the drug more specific toward CCA cells. Finally, the target pathway is highly expressed in human CCA samples.

An unanswered question in this study is how ABC294640 is inhibiting CAFs. Neither TCA or ABC294640 treatment affects CAF cells as expected. In fact, TCA seems to increase the CAFs migration rate, while decreasing histone acetylation and viability. With ABC294640 functionally being the opposite of TCA, you would expect that ABC294640 would at least not affect CAFs cell viability, but it decreases it. This may be due to ABC294640 inhibiting SphK2 in another portion of the cell, such as the cytoplasm or mitochondria[49,50]. This needs to be further studied.

In conclusion, ABC294640 seems to effectively decrease CCA cells' migration and viability by stopping SphK2 from increase histone acetylation and ABC294640 is inhibiting CAFs by some unidentified mechanism. The drug is also able to halt growth and metastasis of CCA tumors. CCA reliance on increased SphK2 activity is supported by SphK2 and S1PR2 levels of the CCA patient samples. More research should be done to determine how ABC294640 can be safely used as a clinical treatment for CCA.

Bibliography

1) Banales, J. M., et al. (2016). "Expert consensus document: Cholangiocarcinoma: current knowledge and future perspectives consensus statement from the European Network for the Study of Cholangiocarcinoma (ENS-CCA)." Nat Rev Gastroenterol Hepatol 13(5): 261-280.

2) Renumathy Dhanasekaran, Alan W. Hemming, Ivan Zendejas, Thomas George, David R. Nelson, Consuelo Soldevila-Pico, Roberto J. Firpi, Giuseppe Morelli, Virginia Clark, Roniel Cabrera. Treatment outcomes and prognostic factors of intrahepatic cholangiocarcinoma. Oncology Reports April 2013 Volume 29 Issue 4 pg. 1259-1267.

3) Nagahashi, M., et al. (2015). "Conjugated bile acid-activated S1P receptor 2 is a key regulator of sphingosine kinase 2 and hepatic gene expression." Hepatology 61(4): 1216-1226.

4) Waseem, D. and P. Tushar (2017). "Intrahepatic, Perihilar and Distal Cholangiocarcinoma: Management and Outcomes." Annals of Hepatology 16(1): 133-139.

5) Malik, V. S., et al. (2013). "Global obesity: trends, risk factors and policy implications." Nat Rev Endocrinol 9(1): 13-27.

6) Zheng, Y., et al. (2018). "Global aetiology and epidemiology of type 2 diabetes mellitus and its complications." Nat Rev Endocrinol 14(2): 88-98.

7) Van Beers, B. E. (2008). "Diagnosis of cholangiocarcinoma." HPB (Oxford) 10(2): 87-93.

8) Sapisochín G, Fernández de Sevilla E, Echeverri J, Charco R. Liver transplantation for cholangiocarcinoma: Current status and new insights. *World J Hepatol*. 2015;7(22):2396-403.

9) Kim MY, Kim JH, Kim Y, Byun SJ. Postoperative radiotherapy appeared to improve the disease free survival rate of patients with extrahepatic bile duct cancer at high risk of loco-regional recurrence. *Radiat Oncol J*. 2016;34(4):297-304.

10) Farhat MH, Shamseddine AI, Tawil AN, et al. Prognostic factors in patients with advanced cholangiocarcinoma: role of surgery, chemotherapy and body mass index. *World J Gastroenterol*. 2008;14(20):3224-30.

11) Sriputtha S, Khuntikeo N, Promthet S, Kamsa-Ard S. Survival rate of intrahepatic cholangiocarcinoma patients after surgical treatment in Thailand. Asian Pac J Cancer Prev. 2013;14(2):1107-10.

12) Witzigmann H, Lang H, Lauer H. Guidelines for palliative surgery of cholangiocarcinoma. *HPB (Oxford)*. 2008;10(3):154-60.

13) Afshar M, Khanom K, Ma YT, Punia P. Biliary stenting in advanced malignancy: an analysis of predictive factors for survival. *Cancer Manag Res*. 2014;6:475-9. Published 2014 Dec 10. doi:10.2147/CMAR.S71111

14) Funasaki, N., et al. (2006). "Micelle formation of bile salts and zwitterionic derivative as studied by two-dimensional NMR spectroscopy." Chem Phys Lipids 142(1-2): 43-57.

15) Jia, W., et al. (2018). "Bile acid-microbiota crosstalk in gastrointestinal inflammation and carcinogenesis." Nat Rev Gastroenterol Hepatol 15(2): 111-128.

16) Chiang, J. Y. (2009). "Bile acids: regulation of synthesis." J Lipid Res 50(10): 1955-1966.

17) Dawson, P. A., et al. (2009). "Bile acid transporters." J Lipid Res 50(12): 2340-2357.

18) Chiang, J. Y. (2013). "Bile acid metabolism and signaling." Compr Physiol 3(3): 1191-1212.

19) Xuefeng Xia, Heather Francis, Shannon Glaser, Gianfranco Alpini, Gene LeSage (2006). "Bile acid interactions with cholangiocytes". The WJG 12(22): 3553-3563.

20) Clouzeau-Girard, H., et al. (2006). "Effects of bile acids on biliary epithelial cell proliferation and portal fibroblast activation using rat liver slices." Lab Invest 86(3): 275-285.

21) Spiegel, S. and S. Milstien (2011). "The outs and the ins of sphingosine-1-phosphate in immunity." Nat Rev Immunol 11(6): 403-415.

22) Nagahashi, M., et al. (2016). "The roles of bile acids and sphingosine-1-phosphate signaling in the hepatobiliary diseases." J Lipid Res 57(9): 1636-1643.

23) Rosenbaum, D. M., et al. (2009). "The structure and function of G-protein-coupled receptors." Nature 459(7245): 356-363.

24) Kwong, E., et al. (2015). "Bile acids and sphingosine-1-phosphate receptor 2 in hepatic lipid metabolism." Acta Pharm Sin B 5(2): 151-157.

25) Hait, N. C., et al. (2007). "Sphingosine kinase type 2 activation by ERK-mediated phosphorylation." J Biol Chem 282(16): 12058-12065.

26) Hait, N. C., et al. (2009). "Regulation of histone acetylation in the nucleus by sphingosine-1-phosphate." Science 325(5945): 1254-1257.

27) Nagahashi, M., et al. (2015). "Conjugated bile acid-activated S1P receptor 2 is a key regulator of sphingosine kinase 2 and hepatic gene expression." Hepatology 61(4): 1216-1226.

28) Liu, R., et al. (2014). "Conjugated bile acids promote cholangiocarcinoma cell invasive growth through activation of sphingosine 1-phosphate receptor 2." Hepatology 60(3): 908-918.

29) Massani, M., et al. (2013). "Isolation and characterization of biliary epithelial and stromal cells from resected human cholangiocarcinoma: a novel in vitro model to study tumor-stroma interactions." Oncol Rep 30(3): 1143-1148.

30) Zhang, X. F., et al. (2017). "Expression pattern of cancer-associated fibroblast and its clinical relevance in intrahepatic."

31) Hirose, Y., et al. (2018). "Generation of sphingosine-1-phosphate is enhanced in biliary tract cancer patients and is associated with lymphatic metastasis." Sci Rep 8(1): 10814.

32) Bertani, H., et al. (2015). "Cholangiocarcinoma and malignant bile duct obstruction: A review of last decades advances in therapeutic endoscopy." World J Gastrointest Endosc 7(6): 582-592.

33) Hatoum D, Haddadi N, Lin Y, Nassif NT, McGowan EM. Mammalian sphingosine kinase (SphK) isoenzymes and isoform expression: challenges for SphK as an oncotarget. *Oncotarget*. 2017;8(22):36898–36929. doi:10.18632/oncotarget.16370.

34) Xiong, Y., et al. (2013). "Sphingosine kinases are not required for inflammatory responses in macrophages." J Biol Chem 288(45): 32563-32573.

35) Lynch, K. R., et al. (2016). "Sphingosine kinase inhibitors: a review of patent literature (2006-2015)." Expert Opin Ther Pat 26(12): 1409-1416.

36) Antoon JW, White MD, Meacham WD, et al. Antiestrogenic effects of the novel sphingosine kinase-2 inhibitor ABC294640. *Endocrinology*. 2010;151(11):5124–5135. doi:10.1210/en.2010-0420

37) Chiang, John. (2013). Bile Acid Metabolism and Signaling. Comprehensive Physiology. 3. 1191-212. 10.1002/cphy.c120023.

38) Kwong, Eric & Li, Yunzhou & Hylemon, Phillip & Zhou, Huiping. (2015). Bile acids and sphingosine-1-phosphate receptor 2 in hepatic lipid metabolism. Acta Pharmaceutica Sinica B. 69. 10.1016/j.apsb.2014.12.009.

39) Gentilini, Alessandra & Pastore, Mirella & Marra, Fabio & Raggi, Chiara. (2018). The Role of Stroma in Cholangiocarcinoma: The Intriguing Interplay between Fibroblastic Component, Immune Cell Subsets and Tumor Epithelium. International Journal of Molecular Sciences. 19. 2885. 10.3390/ijms19102885.

40) Rizvi, S. A. A. and A. M. Saleh (2018). "Applications of nanoparticle systems in drug delivery technology." Saudi Pharm J 26(1): 64-70.

41) Campbell, D. J., et al. (2012). "Novel organotypic culture model of cholangiocarcinoma progression." Hepatol Res 42(11): 1119-1130.

42) Hylemon, P. B., et al. (2017). "Bile acids as global regulators of hepatic nutrient metabolism." Liver Res **1**(1): 10-16.

43) Razumilava, N. and G. J. Gores (2014). "Cholangiocarcinoma." The Lancet **383**(9935): 2168-2179.

44) Weigert, A., et al. (2009). "Sphingosine kinase 2 deficient tumor xenografts show impaired growth and fail to polarize macrophages towards an anti-inflammatory phenotype." Int J Cancer 125(9): 2114-2121.

45) Wallington-Beddoe, C. T., et al. (2014). "Sphingosine kinase 2 promotes acute lymphoblastic leukemia by enhancing MYC expression." Cancer Res 74(10): 2803-2815.

46) Heidi A. Neubauer, et al. (2016) "An oncogenic role for sphingosine kinase 2." Oncotarget, 7(40): 64886 -64900.

47) Britten, C. D., et al. (2017). "A Phase I Study of ABC294640, a First-in-Class Sphingosine Kinase-2 Inhibitor, in Patients with Advanced Solid Tumors." Clin Cancer Res 23(16): 4642-4650.

48) Xiwei Ding, et al. (2019). "Targeting sphingosine kinase 2 suppresses cell growth and synergizes with BCL2/BCL-XL inhibitors through NOXA-mediated MCL1 degradation." Am J Cancer Res 2019;9(3):546-561.

49) Dominguez, G., et al. (2018). "Neuronal sphingosine kinase 2 subcellular localization is altered in Alzheimer's disease brain." Acta Neuropathol Commun 6(1): 25.

50) Graham M. Strub, el al. (2011). Sphingosine-1-phosphate produced by sphingosine kinase 2 in mitochondria interacts with prohibitin 2 to regulate complex IV assembly and respiration. FASEB J. 2011 Feb; 25(2): 600–612.Graham M. Strub

51) Pitman, M. R., et al. (2016). "Recent advances in the development of sphingosine kinase inhibitors." Cell Signal 28(9): 1349-1363.

Vita

Anthony Dean Stillman Graduated with a B.S. in Biology from the University of Washington, 2015.